UNIVERSITY OF GRONINGEN

Non-linear saturated control without velocity measurements for planar, flexible-joint manipulators

by

Thomas Wesselink

A thesis submitted in partial fulfillment for the
degree of Master of Science

in the
Faculty of Science and Engineering
Industrial Engineering and Management

supervised by

Prof. dr. ir. J.M.A. Scherpen

Prof. dr. A.J. van der Schaft

Dr. L.P. Borja Rosales

August 2018

UNIVERSITY OF GRONINGEN

Abstract

Faculty of Science and Engineering
Industrial Engineering and Management

Master of Science

by Thomas Wesselink

In this thesis a constructive procedure for energy-shaping without solving partial differential equations [1] is used to develop control for a planar robot arm with rotational, flexible joints. It is shown that taking the natural damping into consideration can benefit the process of developing control through passivity-based techniques. Furthermore, this work presents a control law that does not use velocity measurements and is by itself fully saturated. All of the resulting control laws are compared against a linear alternative and each other through simulations and tests on an experimental set-up.

Acknowledgements

This thesis is the last theoretical submission for the degree of Master of Science in Industrial Engineering and Management. It concludes a 7 year expedition with many interesting courses that opened my eyes to the world of engineering. In particular I would like to thank prof. dr. ir. Jacquelien Scherpen for the courses in control engineering in both my bachelor's and master's that introduced me to a field that fascinates me beyond any other. Prof. dr. Arjen van der Schaft also built both my knowledge and interest in the field with several courses during my master's that he explained with an enthusiasm and insight almost unparalleled.

During this thesis, prof. Scherpen gave direction to the research and pushed me back on track whenever I came close to veering off course. This guidance, and taking the time out of the fullest schedule I have ever seen to help me was invaluable. Pablo Borja PhD helped me on almost a daily basis, and there has not been a moment where he was not immediately able to help me with my problems. Without his guidance in control theory, mathematics and how to conduct research this thesis would not have even come close to existing. Many, many thanks to both for their help!

Lastly, my parents have supported me in every way during the entirety of my studies. Even before that, they always enabled me to explore my interests and their patience and willingness to answer each of my questions during my youth have caused the start of my academic ambitions. The fact that I was not scolded after, at age five, minutely testing mixes of all the shampoos in the house to develop a super shampoo (and thereby of course ruining all the shampoos) shows a prime example of this. This document is for a large part the result of their efforts and finally a sign of my formal education leading to some results. Thank you both for everything!

Contents

Notation

- All vectors are column vectors and for the scalar function $V(x)$, with $x = (x_1, \ldots, x_n)^\top$, the following derivatives apply:

$$\frac{\partial V}{\partial x}(x) = \begin{bmatrix} \frac{\partial V}{\partial x_1}(x) \\ \vdots \\ \frac{\partial V}{\partial x_n}(x) \end{bmatrix}, \qquad \frac{\partial^2 V}{\partial x^2} = \begin{bmatrix} \frac{\partial^2 V}{\partial x_1^2} & \cdots & \frac{\partial^2 V}{\partial x_n \partial x_1} \\ \vdots & \ddots & \vdots \\ \frac{\partial^2 V}{\partial x_1 \partial x_n} & \cdots & \frac{\partial^2 V}{\partial x_n^2} \end{bmatrix}$$

- The following notation with $x \in \mathbb{R}^n$, $K \in \mathbb{R}^{n \times n}$ is equivalent:

$$x^\top K x \;=\; \|x\|_K^2$$

- A subscripted asterisk outside a bracket means the contents of the bracket are evaluated at a point x^*:

$$\Big[V(x)\Big]_* = \Big(V(x)\Big)_* = V(x)\Big|_* = V(x^*)$$

- Suppose four matrices A, B, C, D are respectively sized $p \times p$, $p \times q$, $q \times p$ and $q \times q$, and that D is invertible. A composite matrix's Schür complement can be found as follows:

$$M := \begin{bmatrix} A & B \\ C & D \end{bmatrix}$$

$$M\Big/D = A - BD^{-1}C \qquad \text{and} \qquad M\Big/A = D - CA^{-1}B$$

- Abuse of notation is often made by leaving out arguments

Chapter 1

Introduction

The focus of this thesis is on designing control for a robot arm with flexible joints. A new, passivity-based, constructive procedure for doing so will be tested. Furthermore, the work in this thesis contributes to literature a case for considering the natural damping and a new saturated form of control without velocity measurements. This introductory chapter will present the concept of (non-linear) control and the challenges that come with it. The definition of the specific problem this thesis aims to solve will delineate within these challenges a more precise focus.

1.1 Control theory

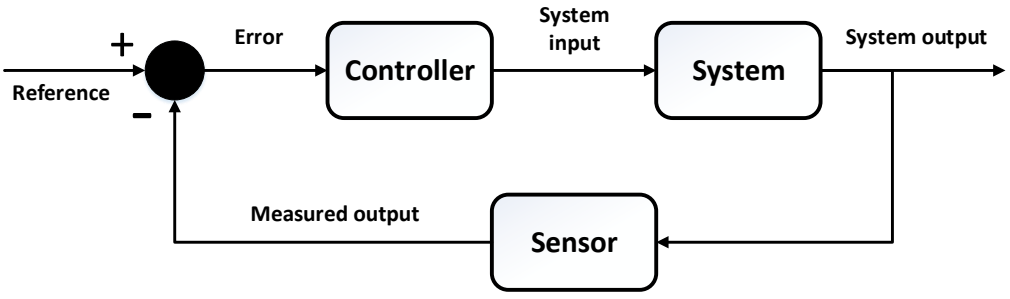

Figure 1.1: A closed-loop feedback control. The output of the system is measured and compared to the desired output. A controller then translates this into an appropriate input.

Engineers dealing with control and automation are concerned with analyzing and controlling bounded parts of their environment. Such a port, when properly defined is

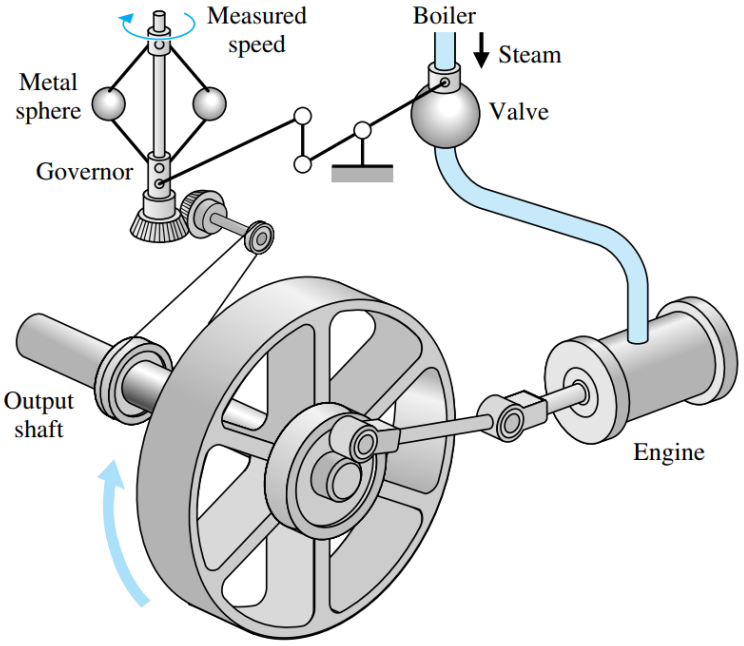

Figure 1.2: The fly-ball governor, invented by James Watt in 1769. The speed of the engine is regulated because at higher speeds, the spinning of the metal spheres raises the governor, decreasing the amount of steam entering the engine. [3]

called a system. These systems often accept an input, produce an output and that what is going inside can be captured in a certain number of states. The goal of the control engineer, is then to device the inputs that, when fed into the system, make the output behave in a desired way. The most prominent form of controllers that are used are closed-loop feedback controllers. In these loops, information about the actual output is compared to the desired output, and the controller then translates the difference into a input signal for the system (see figure 1.1). Although automatic control had been (often unknowingly) used in history, one of the earliest studied examples [2][1] of an automatic (yet fully mechanical) controller was James Watt's fly-ball governor (figure 1.2). Watt developed the device in 1769 to control the speed of steam engines, and it played a large role in enabling the industrial revolution. The field has progressed massively since and modern control systems are often sophisticated entities in which the control law is executed on a computer. The basic elements are however still the same, and the closed-loop feedback principle as seen in Watt's fly-ball governor is currently applied in billions of devices over the world.

[1]For a brief history through early, early twentieth century, and classical control, the reader is referred to this work by Stuart Bennett.

One important development is the mathematical domain in which the analysis of the system's dynamics was performed. Although this analysis initially started with looking at differential equations, developing a simple and useful framework for proving stability of the systems eluded the mathematicians working on the problems. Classical control theory took over around the 1930's with analysis in the Laplace-domain, the systems being described as transfer functions. The 1950's brought modern control techniques, and systems were for the first time described in the state-space notation, which will also be used in this thesis. The state-space of a system is a set of first order differential equations describing the relation between the inputs and outputs of a system, and the solution of each differential equation yields a state: a variable that describes the condition the system is in.

In whatever form, control theory is applicable in any situation in which the output of a system has to be regulated, and in a more and more automated world, the number of this kind of situations is increasing; self-driving cars have to maintain speed and follow a trajectory (fig. 1.3), drones cooperate to create flying light shows (fig. 1.4) and industrial robot arms swing around a factory to produce cars (fig. 1.5).

Figure 1.3: Self driving cars

Figure 1.4: Drones flying in formation

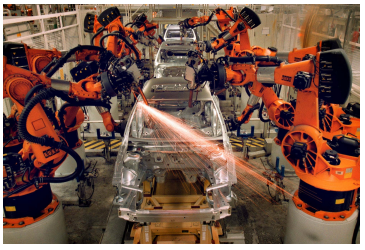

Figure 1.5: Robot arms working on cars

1.2 Non-linear control

The rigorous analysis of systems and ways to control them started with linear systems. James Clerk Maxwell formalized the control principle of Watt's regulator in 1868 [4] (see figure 1.6), and famous theorists as Routh, Sturm and Hurwitz continued this work later. With Nicholas Minorsky and his invention of PID control [5], many of the linear problems became relatively easily solvable. Control of non-linear systems proved harder to crack.

A non-linear system is loosely speaking a system in which the outputs are not directly proportional to its inputs. In other words, the systems dynamics cannot be written as a linear composition of the independent states. The dynamics of these systems behave differently and small differences in the starting conditions or the control signals can generate vastly different outcomes.

Non-linearity also brings other phenomena that do not occur in linear systems. The states can become infinite in finite time, there can be multiple and isolated equilibria, there can be isolated oscillations in which a trajectory may be trapped forever and the number of equilibrium points can change when changing system parameters in a process called bifurcation.

Non-linear systems can be linearized using techniques related to the Taylor expansion but the downside is that all non-linear behaviour is lost. This means that linearized models only partly explain the system's behaviour and additionally only work in a small region around the point of linearization. These models however still work well enough for a lot of practitioners, and the discussion about the need for non-linear models has raised its head multiple times. The analysis of non-linear systems is more complicated than the analysis of their linear counterparts. For linear systems there exist generalized frameworks applicable to every conceivable linear system. A famous quote from Tolstoy's Anna Karenina has once been used to express why non-linear systems are harder to crack: *"Every linear system is linear in the same way, whereas every non-linear system has its own way of being non-linear".* Although for example controllability and observability have been generalized for all non-linear systems, controller synthesis methods have only been successfully developed for certain well delineated classes of systems.

It seems that a generalized method for finding a suitable control law for any non-linear system cannot be possible. However, developing control for well-defined classes of non-linear systems certainly is. The fact that non-linear analysis works in a larger range of motion and can make stronger guarantees about stability than its linear counterpart is a good argument to continue this research. Also, in a significant amount of cases non-linear analysis can yield better performance; this thesis is an example of that.

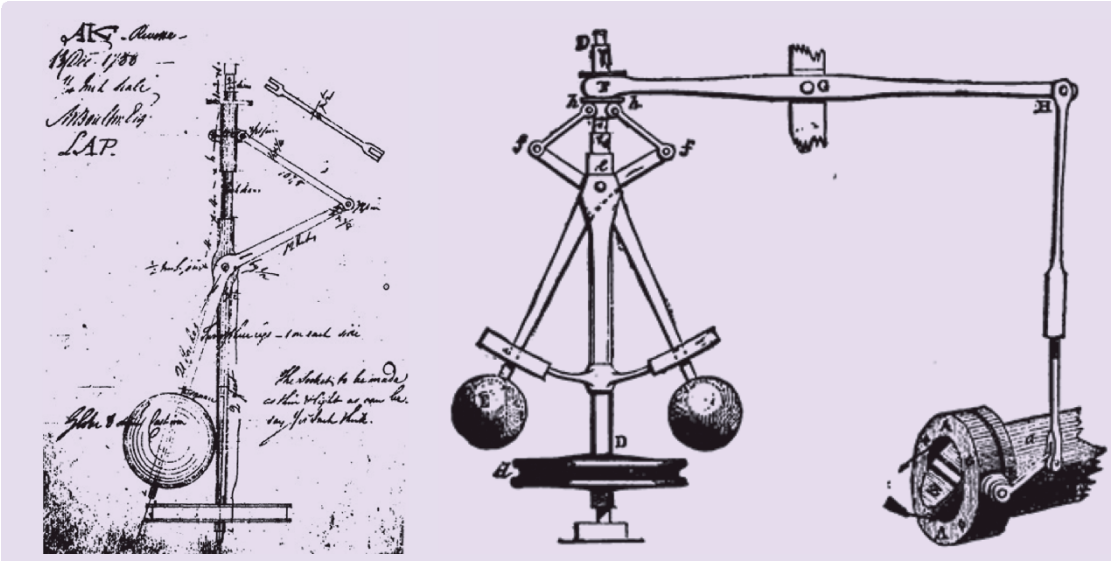

Figure 1.6: Illustrations from Maxwell's work: On governors

1.3 Port-Hamiltonian models and passivity

Whilst topics concerning control and stability are often considered from a mathematical point of view, the engineer needs to keep the practical applications in mind. Control theory is applicable to a broad range of domains, but *energy* is usually the property shared in all of those. This energy is stored, supplied, dissipated and routed between different parts of the physical systems. To model these characteristics, different frameworks exist. The Euler-Lagrangian and Newtonian frameworks are well suited to modeling mechanical systems, but they lack a clear and intuitive representation of the energy. A better alternative in that respect is given by the Hamiltonian framework. It is oriented around the Hamiltonian of a system, which in mechanical systems is the total energy of the system at a certain time.

The concept of port-Hamiltonian further improves this framework. It uses a fixed structure that is based on the interconnection of different parts of the system where the energy flow is represented by *across* and *through* variables. Although not really applicable to this thesis, the connection (of a large number) of parts from different physical domains becomes very convenient through this structure. Another advantage is that it gives a clear and convenient overview of the way parts of the system interact, and where energy is dissipated or added through control inputs.

Passivity is another term closely related to this convenient framework for modelling physical systems. Loosely speaking, a system is passive when it does not generate energy by itself. This means that the energy stored in the system can never be greater than the supplied energy and the energy present in the system at the initial time. All real physical systems automatically adhere to this. The property of passivity turns out to be very useful for control design, the work in this thesis is heavily based on passivity- and energy-based works of Daniel Dirksz [6] and Pablo Borja et al. [1].

Dirksz's work on energy based control design uses the advantage of the energy based representation of PH models to design robust control. The fact that the Hamiltonian can be used as a candidate Lyapunov function, a useful tool to prove stability, is also exploited. Borja's falls under the category of passivity-based control methods. These also exploits the energy-based characteristics of port-Hamiltonian models, for example, they are automatically passive. It aims to change the minimums of energy with regards to the change, and then render the closed loop system stable. Borja's method of PI-PBC is in fact very close to the linear methods with proportional and integral terms, a reassuring nomenclature for practitioners.

1.4 Robot arms and flexible joints

An interesting example of non-linear systems and the area that will be the focus of this thesis is that of robot arms. These arms are extensively used in factories and replace humans in the production process. They can carry loads much larger and yet work at a much higher accuracy than their human counterparts. Often, these arms have rotational joints that allow them to freely move around their workspace. The geometric consequence of having these joints are that the dynamics become non-linear.

The scale and configuration of these arms cause an extra non-linearity: that of flexible joints. In industrial robot arms, transmission systems like harmonic drives and transmission belts allow the link of the robot to be in a slightly different position than the motor, this deflection occurs in an elastic manner. A second possibility is that the length of the arm is so large that it bends slightly causing the end of the manipulator to be at a different angle than the beginning and therefore the motor.

1.5 Problem formulation

A way to tackle the problem of designing control for non-linear systems is passivity-based control. The energy-balance of the system has certain characteristics that can be exploited to design control laws that provide desired performance. However, most techniques associated to this method require solving differential equations. This is often a difficult and time-consuming process. Borja et al. [1] devised a procedure to use passivity without solving partial differential equations. This procedure will be applied to the non-linear flexible-joint robotic manipulators as discussed in the previous section. Its usefulness as a way to develop robust and efficient control techniques will be tested.

Furthermore, in theoretical work, the choice is often made to include the velocity in the control law. In practice, velocity cannot be measured directly. The velocity measurements are obtained by differentiating the position measurements over time. Since the resolution of position measurements are limited (often by the amount of slips on an encoder disk), these measurements already have a certain error. This error will amplify when the position measurements are used to calculate the velocity. Another problem is that these methods and sensors are expensive. It is therefore desirable to be able to control a robot arm without these measurements.

A third problem to which this thesis aims to provide a solution is that in practice, systems can often only handle inputs with a limited amplitude. A reasonable input for a robot arm is an electric current expressed in Ampère. If the controller output is a current that is too strong, the motors in the arm might be damaged. Control signals are therefore often saturated, which often means that any signal exceeding a certain threshold is cut off. The relatively unsophisticated way to handle strong signals can cause vibration and trouble the analysis. The effects are often largely ignored and if the proof that a control law works without saturation is given the research is often concluded without further thought about the applications.

Lastly, the natural damping of systems is often kept out of consideration in theoretical work about control. In reality, a form of damping is almost always present. In robot arms, this damping comes from friction between different parts or the air resistance caused by moving the arm through its environment. The effects of damping are therefore not always extensively researched and when it is, it is seen as a nuisance and negating

its effect is often a priority. In this thesis it is shown, that damping can have an enabling effect as well, and including it in research can be worth the trouble.

1.6 Thesis outline

From this point on, the challenges discussed will be treated in the following order. A preliminary chapter will explain the port-Hamiltonian framework in which the systems are considered, the notions of stability and passivity and methods to prove the requirements for these notions are satisfied, and passivity-based control. The next chapter, Chapter 3, will treat the way flexible-joint manipulators can be modelled. Chapter 4 will test Borja et al.'s [1] constructive procedure on the robot arm. Chapter 5 will explain how considering natural damping can help in this case and Chapter 6 will remove velocity measurements from the control law and saturate the signals. The last chapter, Chapter 7, will present results about the rejection of external disturbances. Chapter 8 features a discussion of the work in this thesis and possibilities for further research.

Chapter 2

Preliminaries

This chapter will present an outline of the theoretical background of the methods used in this thesis. The chapter will feature a section about port-Hamiltonian systems, since the arm will be modelled using this framework. As the goal of this thesis is to develop a stable control, a definition of stability as well as a summary of methods to prove stability will also be given. Finally passivity-based control, the method of control development the techniques in this thesis are based on, will be explained.

2.1 The port-Hamiltonian framework for mechanical systems

The analysis of physical and especially mechanical systems has taken place mostly within the Lagrangian or Hamiltonian frameworks. The Euler-Lagrangian equations are given as

$$\frac{d}{dt}\left(\frac{\partial L}{\partial \dot{q}}(q,\dot{q})\right) - \frac{\partial L}{\partial q}(q,\dot{q}) = \tau \tag{2.1}$$

in which $L = T(q,\dot{q}) - V(q)$ is the Lagrangian of the system and exists of the kinetic energy T and potential energy V. $q = (q_1, \ldots, q_n)$ are the generalized coordinates for a system with n degrees of freedom. The notations $\frac{\partial L}{\partial q}$ and $\frac{\partial L}{\partial \dot{q}}$ represent the column vectors of partial derivatives of L with respect to the generalized coordinates q or its derivatives $\dot{q}$. The vector τ incorporates the (generalized) forces acting on each state

of the system into the model. The kinetic energy T takes in mechanical systems the following form:

$$T(q, \dot{q}) = \frac{1}{2}\dot{q}^\top M(q)\dot{q} \tag{2.2}$$

in which the mass-inertia matrix $M(q)$ is symmetric and positive-definite for all q. The generalized momenta $(p_1, \ldots, p_n)$ are defined as $p = \frac{\partial L}{\partial \dot{q}}$ and for mechanical systems are given by:

$$p = M(q)\dot{q} \tag{2.3}$$

For the Hamiltonian framework, the Hamiltonian can be found from the Lagrangian by applying the Legendre transformation:

$$H = \dot{q}\frac{\partial L}{\partial \dot{q}} - L$$

resulting for mechanical systems in $H = T + V$. Using (2.3) and the fact that $M(q)$ is symmetric the Hamiltonian can be rewritten in terms of the coordinates and momenta:

$$H(q, p) = \frac{1}{2}p^\top M^{-1}(q)p + V(q) \tag{2.4}$$

The Hamiltonian conveniently represents the total energy of the system and allows for the Hamiltonian equations of motion. In these equations, the n second-order equations of (2.1) are replaced by $2n$ first-order equations:

$$\begin{aligned} \dot{q} &= \frac{\partial H}{\partial p}(q, p) \\ \dot{p} &= -\frac{\partial H}{\partial q}(q, p) + \tau \end{aligned} \tag{2.5}$$

These equations can be generalized to:

$$\begin{aligned}\dot{q} &= \frac{\partial H}{\partial p}(q,p), \qquad q,p \in \mathbb{R}^n \\ \dot{p} &= -\frac{\partial H}{\partial q}(q,p) + B(q)u, \qquad u \in \mathbb{R}^m \\ y &= B^\top(q)\frac{\partial H}{\partial p}(q,p), \qquad y \in \mathbb{R}^m\end{aligned} \tag{2.6}$$

where $B(q)$ is the input force matrix with $B(q)u = \tau$. Considering that m is the amount of inputs, if $m < n$ the system is underactuated and not all momenta can directly be influenced by the input u. If $m = n$ and the matrix $B(q)$ is invertible for all q the system is fully actuated. These equations can be further generalized for any local coordinates x on an n-dimensional state space manifold $\mathcal{X}$ whilst including energy dissipation. The equations of motion in (2.7) are, under the assumptions of (2.8), in port-Hamiltonian (PH) form (introduced by Maschke and van der Schaft in [7]).

$$\begin{aligned}\dot{x} &= \big(J(x) - R(x)\big)\frac{\partial H}{\partial x}(x) + g(x)u \\ y &= g^\top(x)\frac{\partial H}{\partial x}(x), \qquad y \in \mathbb{R}^m\end{aligned} \tag{2.7}$$

$J(x)$ is the $n \times n$ interconnection matrix that shows the way energy travels between different elements of the system. It is assumed to be skew-symmetric. $R(x)$ is a positive definite, symmetric matrix called the damping matrix. This damping matrix governs the energy dissipation of the system.

$$\begin{aligned}J(x) &= -J^\top(x) \\ R(x) &= R^\top(x) \geq 0\end{aligned} \tag{2.8}$$

PH systems can describe many (non-linear) systems including mechanical, electrical, electro-mechanical and thermal systems. It is especially useful to describe complex systems since parts of the model can be split and connected through the interconnection matrix. More information, including more detailed explanations of the material in this section, can be found in [8], [7].

2.2 Stability and passivity

2.2.1 Stability

Stability is an important concept in dynamical systems that describes certain aspects of their behavior. In particular, stability tells one about the states of a system over time, and whether or not they are contained in a certain region. A more precise definition of stability in the sense of Lyapunov [9] follows:

Definition 2.1. An equilibrium point $x^* \in \mathbb{R}^n$ is called

- *stable*, if for every $\epsilon > 0$ there exists a $\delta > 0$ such that if $\|x_0 - x^*\| < \delta$ then $\|x(t; x_0) - x^*\| < \epsilon$ for all $t \geq 0$.
- *asymptotically stable*, if x^* is stable and there exists a $\delta > 0$ such that $\|x_0 - x^*\| < \delta$ implies that $\lim_{t\to\infty} x(t; x_0) = x^*$.
- *globally asymptotically stable*, if x^* is stable and for every x_0, $\lim_{t\to\infty} x(t; x_0) = x^*$.
- *unstable*, if x^* is not stable.

The notation $x(t; x_0)$ indicates the trajectory of state x over time t with initial conditions x_0.

To prove whether or not an equilibrium is (asymptotically) stable, the methods in this thesis will rely heavily on Lyapunov's second method. Additionally, Barbalat's lemma is used to analyze the behaviour of certain functions as $t \to \infty$. Both will be explained in the next sub-sections.

Lyapunov's second method

Aleksandr Lyapunov (1867 - 1918) was a Russian mathematician who developed several methods to investigate the stability of equilibrium points. His second method, also known as Lyapunov's direct method, relies on finding a function that does not increase along the solutions: a *Lyapunov function*.

Definition 2.2. Let $\Omega \subset \mathbb{R}^n$ be a subset containing an open neighborhood of equilibrium point x^*. A function $V : \Omega \to \mathbb{R}$ is called a *Lyapunov function* for equilibrium point x^* if:

1. V is continually differentiable.
2. V has a unique minimum in x^*, and $V(x^*) = 0$.
3. For all $x \in \Omega$, V satisfies the following inequality:

$$\dot{V}(x) = \sum_{i=1}^{n} \frac{\partial V}{\partial x_i} \dot{x}_i \leq 0$$

Remark 2.3. For systems with multiple states, as will be encountered in this thesis showing a potential Lyapunov function has a unique minimum can be performed as follows: a function V has a unique minimum in x^* if:

1. $\frac{\partial V}{\partial x}(x)\Big|_{x^*} = \mathbb{0}^{n \times 1}$
2. $\frac{\partial^2 V}{\partial x^2}(x)\Big|_{x^*} > 0$ (is positive definite)

where $\frac{\partial V}{\partial x}$ is the vector of partial derivatives of V with respect to all states x and $\frac{\partial^2 V}{\partial x}$ the Hessian matrix of V with respect to states x.

Stability can be investigated using a Lyapunov function using the following theorem (for which the proof can be further studied in [9]):

Theorem 2.4. *Lyapunov's direct method: Consider a system as in* (2.7) *without inputs (i.e.* $u = 0$*) defined on* $\mathbb{R}^n$ *with equilibrium point* x^**. If there exists a Lyapunov function* V *on an open neighborhood* $\Omega \subset \mathbb{R}^n$ *of* x^**, then the equilibrium point* x^* *is stable. Furthermore, if* $\dot{V}(x) < 0$ *for all* $x \in \Omega \setminus \{x^*\}$*, then* x^* *is asymptotically stable.*

Lasalle's invariance principle

A problem that often arises is that asymptotic stability is often hard to prove using only Lyapunov's direct method. As explained in the last subsection, a point is only asymptotically stable if the Lyapunov function is negative definite. In practice, $\dot{V}$ rarely depends on all states. In this case, LaSalle's invariance principle can often be used to prove asymptotic stability. First, an important notion for this principle is defined: the invariant set.

Definition 2.5. A set $\mathcal{G} \subset \mathbb{R}^n$ is called an invariant set for (2.7) without inputs (i.e. $u = 0$) if every solution of (2.7) with initial condition in $\mathcal{G}$, is contained in $\mathcal{G}$.

This allows stating LaSalle's invariance principle:

Theorem 2.6. *Lasalle's invariance principle: Let $\mathcal{K}$ be a compact invariant set in the neighborhood of x^* for (2.7) without input (i.e. $u = 0$). Let V be a continuously differentiable function on $\mathcal{K}$ with $\dot{V} \leq 0$. Define $\mathcal{S} := \left\{x \in \mathbb{R}^n \;\middle|\; \dot{V} = 0\right\}$ and $\mathcal{G}$ the largest invariant set in $\mathcal{S}$. Then for every $x_0 \in \mathcal{K}$, the solutions of x converges to $\mathcal{G}$, i.e.* $\lim_{t\to\infty} d(x(t; x_0), \mathcal{G}) = 0$.

Loosely speaking, if a Lyapunov function with a semi-negative definite time derivative is found, all solutions will converge to the largest invariant set contained in the set where $\dot{V} = 0$. When the equilibrium point x^* is shown to be the largest invariant set in $\mathcal{S}$, it can be concluded that x^* is asymptotically stable.

A useful corollary (but proven before the introduction of LaSalle's invariance principle) is Barbashiin's theorem:

Corollary 2.7. *Let x^* be an equilibrium point and V a Lyapunov function on a domain $\mathcal{D}$ containing x^*. Let $S = \left\{x \in \mathcal{D} \;\middle|\; \dot{V} = 0\right\}$ and suppose no solution can stay identically in S except the trivial solution. Then, the origin is asymptotically stable.*

The proofs and more detailed information about these methods can be further studied in [9], [10].

Barbalat's lemma

Lyapunov's direct method and LaSalle's invariance principle can be used for non-autonomous systems. That is, systems of which the dynamics do not directly rely on time (t). Barbalat's lemma (for proof see [9]) is especially useful for systems of which the dynamics do explicitly rely on time (time-varying or autonomous systems), but has uses elsewhere too, as is shown throughout this thesis.

Theorem 2.8. *Barbalat's lemma: Suppose $f(t) \in C^1(a, \infty)$ and $\lim_{t\to\infty} f(t) = a$ where $a < \infty$. If $\dot{f}$ is uniformly continuous, then $\lim_{t\to\infty} \dot{f}(t) = 0$.*

This is a useful property because of the following corollary:

Corollary 2.9. *If a function $f(t) : \mathbb{R}^n \to \mathbb{R}$ is twice differentiable, has a finite limit, and its second derivative is bounded then $\dot{f}(t) \to 0$ as $t \to \infty$.*

Another useful corollary [11] (to the same extent) can be stated as follows:

Corollary 2.10. *If a function $f(t) : \mathbb{R}^n \to \mathbb{R}$ satisfies the following conditions:*

- *$f(t)$ is lower bounded*
- *$\dot{f}(t)$ is negative semi-definite*
- *$\dot{f}(t)$ is uniformly continuous*

then $\dot{f}(t) \to 0$ as $t \to \infty$

2.2.2 Dissipativity and passivity

Dissipativity and passivity (see [12], [13]) are concepts that, in the context of the physical systems treated in this thesis, are closely related to the energy-balance and flows in the system. Roughly speaking, a system is dissipative if it releases (dissipates) energy to the environment. Passive systems are a subclass of dissipative systems which do not store more energy than is supplied to it (it does not generate energy by itself). To more formally define these concepts, consider a general state-space system:

$$\Sigma : \begin{aligned} \dot{x} &= f(x, u) \\ y &= h(x, u) \end{aligned} \tag{2.9}$$

In this system with input $u \in \mathbb{R}^m$, output $y \in \mathbb{R}^p$ and $x = (x_1, \ldots, x_n)^\top$ the coordinates for an n-dimensional state space manifold $\mathcal{X}$, the scalar function $s\big(u(t), y(t)\big)$ is called the supply rate.

Definition 2.11. A state-space system as in (2.9) is:

- **dissipative** with respect to supply rate s if there exists a function $S : \mathcal{X} \to \mathbb{R}^+$ (called the storage function) such that for all $x_0 \in \mathcal{X}$, all $t_1 \geq t_0$ and all input functions u:
$$S\big(x(t_1)\big) \leq S\big(x(t_0)\big) + \int_{t_0}^{t_1} s\big(u(t), y(t)\big)\ \mathrm{d}t$$
- **passive** if it is dissipative with respect to supply rate s(u,y) $= u^\top y$, i.e.
$$S\big(x(t_1)\big) \leq S\big(x(t_0)\big) + \int_{t_0}^{t_1} u^\top y\ \mathrm{d}t$$

For Hamiltonian systems without damping (i.e. (2.7) with $R(x) = 0$), passivity comes natural. Because of the form of the output $y = B^\top(q)\dot{q}$ the energy-balance is as follows:

$$\dot{H}\big(q(t), p(t)\big) = u^\top(t)y(t)$$

showing that a Hamiltonian system is passive according to definition (2.11) when H is non-negative. In this approach, the Hamiltonian H is used as storage function. The above system is (when H is non-negative) in fact lossless, a strong form of passivity if the time-derivative of the storage function is equal to (=) instead of less than or equal ($\leq$) to the supply rate. For systems like (2.7) with damping, the energy balance takes the following form:

$$\dot{H}\big(q(t), p(t)\big) = u^\top(t)y(t) - \left(\frac{\partial H}{\partial x}\big(x(t)\big)\right)^\top R\big(x(t)\big)\frac{\partial H}{\partial x}\big(x(t)\big) \leq u^\top(t)y(t)$$

showing again that the system is passive (but not lossless) when H is non-negative.

2.3 Passivity-based control

The notion of passivity enables the effective design of control methods through a technique called passivity-based control [13] (PBC). The groundwork for PBC was laid by Jan C. Willems [12] and among others extended by Hill and Moylan [14]. In the currently used variants of this technique, the input is used to passivize the system to be controlled with respect to a storage function that has a minimum at the desired equilibrium. This renders the equilibrium point stable. Usually, damping is then injected to ensure the equilibrium becomes asymptotically stable.

In this thesis the focus is on classical PBC, meaning that a storage function is selected beforehand (in this case the Hamiltonian), and a control law is then designed to make the storage function's time-derivative negative(-semi) definite. Additionally, interconnection and damping assignment passivity-based control (IDA-PBC) will be used to explain the success of some alternative control method. IDA-PBC is part of a class of PBC methods that aim to achieve a certain closed-loop structure instead of a desired storage function. The energy functions that are valid for that structure are then given by a set of partial differential equations.

2.3.1 Classical PBC

In the version of classical PBC used in this thesis, found by Borja et al. [1], the Hamiltonian acts as natural storage function since it represents the energy of the system. The goal is to find a control law:

$$u = a(x) + v$$

to change the system into a system with PH structure but a changed Hamiltonian:

$$\begin{aligned} \dot{x} &= (J(x) - R(x)) \frac{\partial H_d}{\partial x}(x) + g(x)v \\ y &= g(x)^\top \frac{\partial H_d}{\partial x}(x) \end{aligned}$$

The desired Hamiltonian H_d is chosen so that it has a minimum at desired equilibrium x^*. This leads to the following time-derivative:

$$\dot{H}_d = -\left(\frac{\partial H_d}{\partial x}\big(x(t)\big)\right)^\top R\big(x(t)\big)\frac{\partial H_d}{\partial x}\big(x(t)\big) + y^\top v$$

Since H is non-increasing, the system is stable. v can now be chosen so that the system becomes asymptotically stable. Usually, a form of $v = K(x)y$, with $K(x)$ a positive definite matrix, can be used.

2.3.2 IDA-PBC

For IDA-PBC (see [15]), there exists not only a desired Hamiltonian H_d, but also a desired structure consisting of J_d and R_d. This entire desired closed-loop system is given by:

$$\begin{aligned} \dot{x} &= (J_d(x) - R_d(x)) \frac{\partial H_d}{\partial x}(x) \\ y &= g(x)^\top \frac{\partial H_d}{\partial x}(x) \end{aligned}$$

In which the constraints on $J(x)$ and $R(x)$ given in (2.8) have to be satisfied by $J_d(x)$ and $R_d(x)$ as well. Any function that satisfies the following partial differential equations can be used as H_d:

$$g^\perp(x)\left([J_d(x) - R_d(x)]\frac{\partial H_d}{\partial x}(x) - [J(x) - R(x)]\frac{\partial H}{\partial x}(x)\right) = 0$$

where $g^{\perp}$ is the left annihilator of $g(x)$. This yields:

$$\dot{H}_d = -\left(\frac{\partial H_d}{\partial x}\big(x(t)\big)\right)^{\top} R\big(x(t)\big)\frac{\partial H_d}{\partial x}\big(x(t)\big)$$

Here LaSalle's invariance principle is often used to prove that the resulting closed loop system has x^* as an asymptotically stable equilibrium.

2.4 Linear Quadratic Regulators

As a counterpart of the methods discussed in this thesis, infinite horizon linear quadratic regulators (LQRs) will be used to compare the performances of non-linear and linear methods. The LQR is a control law that provides optimal control based on a linear quadratic cost function (see for example [16]). It is always based on a linear system:

$$\dot{x} = Ax + Bu$$

and a cost function of the following form:

$$J = \int_0^{\infty} \left(x^{\top}Qx + u^{\top}Ru + 2x^{\top}Nu\right)\,\mathrm{d}t$$

The optimal control is then given by:

$$u = -R^{-1}\left(B^{\top}P + N^{\top}\right)x$$

where P is found by solving the algebraic Riccati equation:

$$A^{\top}P + PA - (PB + N)R^{-1}(B^{\top}P + N^{\top}) + Q = 0$$

This concludes the preliminary section on the theory needed for the following chapters. For more in-depth explanation and proofs the reader is referred to the citations at the respective theorems.

Chapter 3

Flexible-joint manipulators

This chapter describes the robot arm to be controlled. Although the model that is developed describes robots with flexible joints in general, specific focus will be on the *Quanser 2-DOF Serial Flexible Joint* robot (see figure 3.1). This is the arm used as an experimental set-up to further evaluate the developed control. The Quanser arm has two set-ups, one with rigid and one with flexible joints, which can be alternated between by placing struts between two distinct parts of the joint. Although the focus is on the flexible case, because of this adaptability, the (closely related) rigid joint model will also be developed in order to perform additional tests.

Figure 3.1: The Quanser 2-DOF Serial Flexible Joint

3.1 Flexible joints

For the flexible case, the following (standard [17], [18]) assumptions are made [19]:

- All joints are of rotatory type.
- The displacement between each link and motor is small, a linear model is therefore used for the springs.
- The center of mass of each of motor is located somewhere on the motor's rotational axis.
- The angular velocity of the motors is only due to their own spinning.

For an arm with n links and joints we denote q_{l_i} for the angular position of link i and q_{m_i} for the angular position of motor i. $q_l, q_m, p_l, p_m \in \mathbb{R}^n$ are the respective vectors of link and motor (angular) positions and momenta.

$$q = \begin{bmatrix} q_l \\ q_m \end{bmatrix} \in \mathbb{R}^{2n}$$

the vector of all angular positions. Motor 1 is considered the base of the arm and link 1 is attached to this motor. Motor 2 is then mounted at the end of link 1, and controls link 2. This process repeats itself until link n.

To find the Hamiltonian, it is useful to first list all energies of the arm:

- *Kinetic energy of the links:* $T_l(q_l, \dot{q}_l) = \frac{1}{2}\dot{q}_l^\top M_l(q_l)\dot{q}_l$ where $M_l(q_l) = M_l^\top(q_l) > 0$ is the link's mass-inertia matrix.
- *Kinetic energy of the motors:* $T_m(q_m) = \frac{1}{2}\dot{q_m}^\top M_m \dot{q_m}$ where $M_m = M_m^\top > 0$ is the motor's mass-inertia matrix.
- *Potential energy due to gravity:* Not applicable. Gravity does not affect the system since rotation only occurs in the horizontal plane.
- *Potential energy due to elastic joints:* $V(q_l, q_m) = \frac{1}{2}(q_m - q_l)^\top K_s(q_m - q_l)$ where K_s is the diagonal positive-definite spring matrix.

The Hamiltonian can now be expressed as:

$$H(q,p) = \frac{1}{2}\dot{q}_l^\top M_l(q_l)\dot{q}_l + \frac{1}{2}\dot{q}_m^\top M_m \dot{q}_m + \frac{1}{2}(q_l - q_m)^\top K_s(q_l - q_m)$$

Keeping in mind $p = M\dot{q}$ the Hamiltonian rewrites to:

$$H(q,p) = \frac{1}{2}p^\top M^{-1}p + \frac{1}{2}(q_l - q_m)^\top K_s(q_l - q_m) \tag{3.1}$$

with

$$M = \begin{bmatrix} M_l(q_l) & 0 \\ 0 & M_m \end{bmatrix} = M^\top > 0$$

Until explicitly stated otherwise, damping will not be considered (i.e. $R = 0$, see (2.7)). Since the links cannot be directly influenced the system is underactuated and the model becomes:

$$\begin{bmatrix} \dot{q} \\ \dot{p} \end{bmatrix} = \begin{bmatrix} 0 & I \\ -I & 0 \end{bmatrix} \begin{bmatrix} \frac{\partial H}{\partial q} \\ \frac{\partial H}{\partial p} \end{bmatrix} + \begin{bmatrix} 0 \\ B \end{bmatrix} u, \qquad \text{with } B = \begin{bmatrix} 0_{n\times m} \\ I_{n\times m} \end{bmatrix} \tag{3.2}$$

For the 2-link experimental set-up the mass-inertia matrices are as follows:

$$M_l(q_l) = \begin{bmatrix} a_1 + a_2 + 2b\cos q_{l_2} & a_2 + b\cos q_{l_2} \\ a_2 + b\cos q_{l_2} & a_2 \end{bmatrix} \qquad M_m = \begin{bmatrix} I_{m_1} & 0 \\ 0 & I_{m_2} \end{bmatrix}$$

with constants:

$$\begin{aligned} a_1 &= m_1 r_1^2 + m_2 l_1^2 + I_1 \\ a_2 &= m_2 r_2^2 + I_2 \\ b &= m_2 l_1 r_2 \end{aligned}$$

where m_i, l_i and I_i are the mass, length and inertia of link i, r_i is the distance of the center of mass of link i to its point of rotation and I_{m_1} the inertia of motor i exact values can be found in Table 3.1. In this table, the parameters corresponding to the natural damping, D_l (for the links) and D_m (for the motors) were found through experimentation. The simulated results were compared to the experimental results under identical circumstances and the values for D_l and D_m were chosen so that the two results resembled each other the most.

i	1	2
m_i	0.5	1
l_i	0.343	0.275
r_i	0.2	0.25
I_i	0.01	0.01
I_{m_i}	0.001	0.001
K_{s_i}	9.0	4.0
D_l	0.001	0.001
D_m	0.01	0.01

Table 3.1: Parameters of experimental set-up by Quanser [6]

3.2 Rigid joints

The rigid case is similar to the flexible case with a notable absence of potential energy due to flexible joints. Since the joint and link are always aligned (i.e. $q_l = q_m$ a single angular position sufficiently describes both joint and link positions. $q_m, p \in \mathbb{R}^n$ are the link (and motor) angular positions and momenta. Because all states can now be actuated we have the following model:

$$\begin{bmatrix} \dot{q}_m \\ \dot{p} \end{bmatrix} = \begin{bmatrix} 0 & I \\ -I & 0 \end{bmatrix} \begin{bmatrix} \frac{\partial H}{\partial q_m} \\ \frac{\partial H}{\partial p} \end{bmatrix} + \begin{bmatrix} 0 \\ B \end{bmatrix} u, \qquad \text{with } B = I_{n\times m} \tag{3.3}$$

with Hamiltonian:

$$H = \frac{1}{2}\dot{q}_m^\top M_r(q_m)\dot{q}_m = \frac{1}{2}p^\top M_r^{-1}(q_m)p \tag{3.4}$$

and:

$$M_r(q_m) = M_l(q_m) + M_m = \begin{bmatrix} a_1 + a_2 + 2b\cos q_{m_2} & a_2 + b\cos q_{m_2} \\ a_2 + b\cos q_{m_2} & a_2 \end{bmatrix} + \begin{bmatrix} I_{m_1} & 0 \\ 0 & I_{m_2} \end{bmatrix}$$

3.3 Assumptions and comparison with linear control laws

In order to properly use LaSalle it is assumed that the initial conditions $(q_0, p_0)^\top = \big(q(t_0), p(t_0)\big)^\top$ will always be in a compact neighborhood around the desired equilibrium point.

Definition 3.1. A topological space X is called locally compact if every point x in X has a compact neighborhood, so that there exist an open set S and a compact set C such that $x \in S \subseteq C$

All designed controllers will be tested in both a simulation and experimental environment. The model as described in chapter 3 with parameters as in 3.1 will be used for the simulations, and the Quanser 2-DOF Serial Flexible-Joint experiment will be used for the experiments. In every situation the reference signals will be a step function to 1 rad for link 1, and a step function to -1 rad for link 2, the step occuring at $t = 0$.

Since in the experimental set-up, the control signals are cut off above 1.2 and below -1.2 to protect the motors, the same saturation is applied in the simulations. The control signals are always shown in their original form, without saturation.

As a baseline, a linear quadratic regulator (LQR) based on the linearization of the model around $(q_{l_1}, q_{l_2}, p) = (1, -1, 0)$ is used to test the performance of the non-linear control laws against a linear one. The LQRs minimize the following quadratic cost function:

$$\int_0^\infty x^\top Q x + u^\top R u + 2x^\top N u \, \mathrm{d}t \quad \text{with:} \quad Q, R = I, \; N = 0$$

It is worth noting that the LQR uses velocity measurements.

Rigid-joint LQR results

The results show that in the rigid case, the LQR performs well. The positions are driven to their reference signal between 2 and 4 seconds, with small overshoot and no notable oscillations. A small steady-state error exists in the experimental results, see figure 3.2. This is a performance that is relatively good, the positions converge fast and there is little to no overshoot.

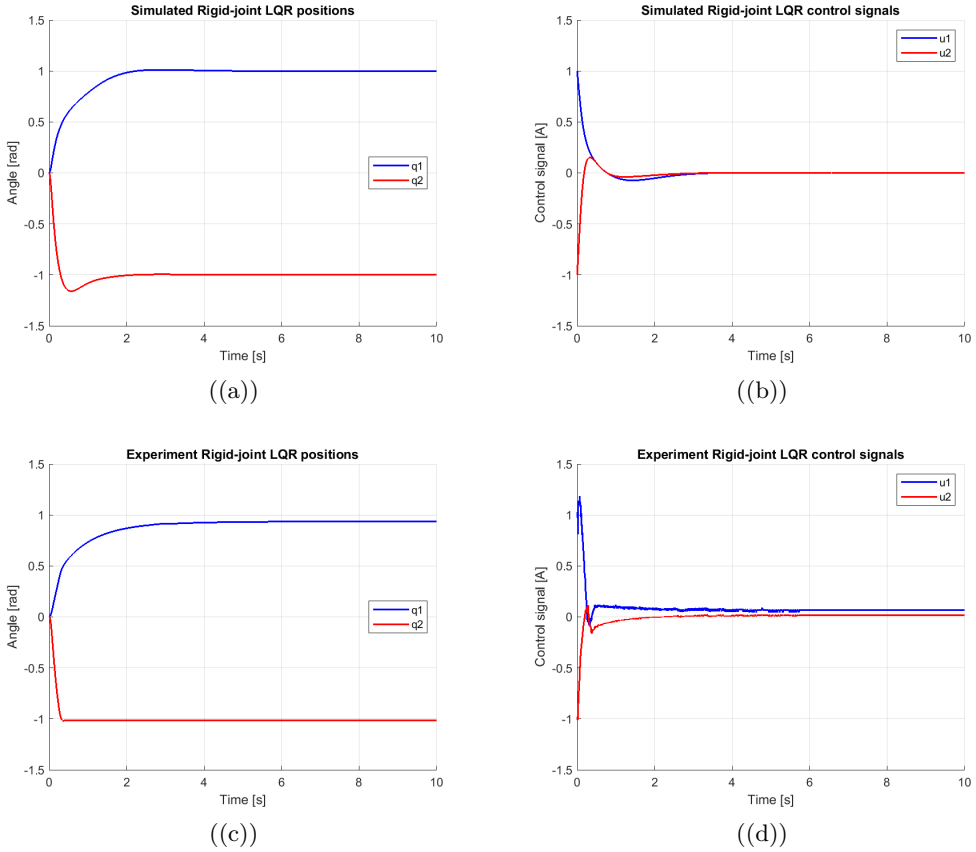

Figure 3.2: Simulated and experimental positions and control signals for LQR on rigid-joint arm

Flexible-joint LQR results

In the flexible case the LQR has more difficulty in driving the positions to their desired points. The convergence is noticeably slower and the links oscillate around the motors. Convergence, barring again a steady-state error in the experimental set-up, happens in approximately 10 seconds. See figure 3.3. The performance of the LQR in the flexible case is noticeably worse than in the rigid case. The fact that the system becomes underactuated and more complex all together when the joints are flexible explains part of this.

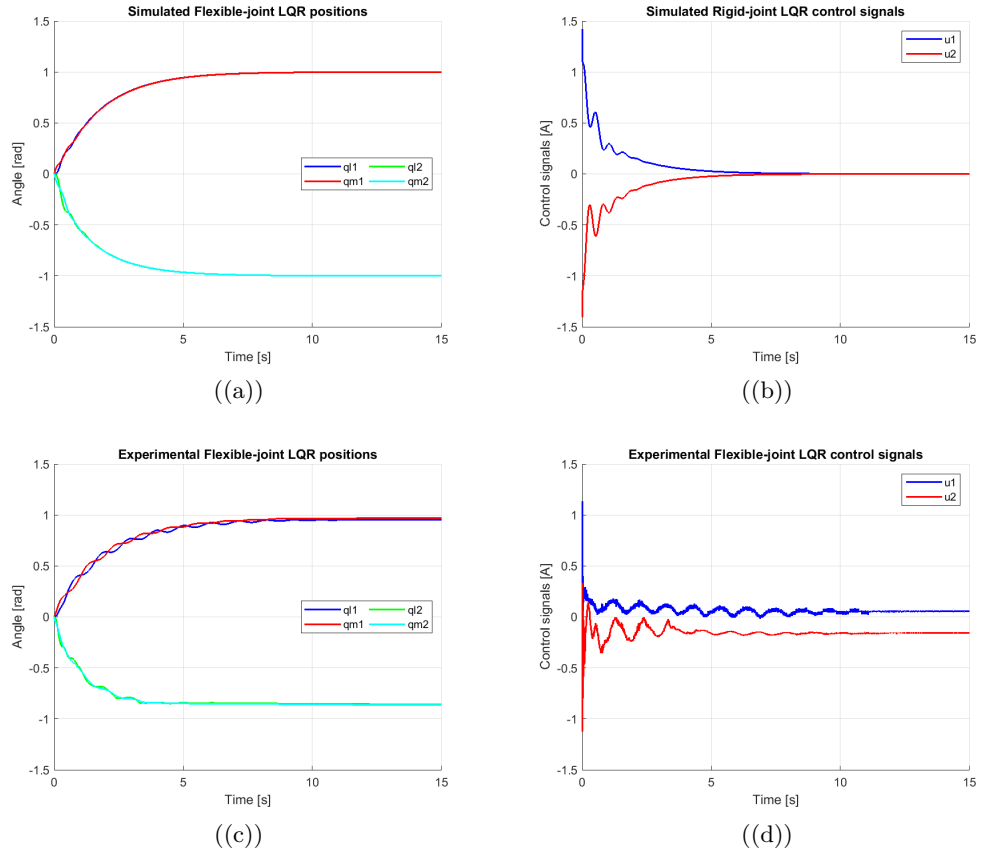

Figure 3.3: Simulated and experimental positions and control signals for LQR on flexible-joint arm

An interesting philosophy about the worse performance of the LQR in the flexible case is that the flexible case is, in a sense, more non-linear. The added complexity caused by the flexibility in the joints reduces the similarity of the non-linear model to the linearized model. The non-linear control laws developed in the rest of this thesis might be more beneficial in the flexible case than in the rigid case.

Chapter 4

Passivity-based PI control

The approach of passivity-based control in this thesis is to change the Hamiltonian to a desired Hamiltonian with a strict minimum at the desired equilibrium. Damping is then injected to make the equilibrium asymptotically stable. In this chapter, a control law for the rigid case will first be explained to illustrate the method with a simpler system. The flexible case will be treated afterwards.

4.1 Rigid case

Proposition 4.1. *The control law* $u := -K_I\tilde{q}_m - K_P\dot{q}_m$ *renders the rigid system asymptotically stable.*

Proof. For the rigid case, the system as in (3.3) with Hamiltonian (3.4) is considered. The passive output y is identified first:

$$\dot{H}(q_m,p) = \left(\frac{\partial H}{\partial x}\right)^\top \begin{bmatrix} \dot{q}_m \\ \dot{p} \end{bmatrix} = \begin{bmatrix} \left(\frac{\partial H}{\partial q_m}\right)^\top & \left(\frac{\partial H}{\partial p}\right)^\top \end{bmatrix} \begin{bmatrix} \dot{q} \\ \dot{p} \end{bmatrix} =$$

$$\begin{bmatrix} \left(\frac{\partial H}{\partial q_m}\right)^\top & \left(\frac{\partial H}{\partial p}\right)^\top \end{bmatrix} \left(\begin{bmatrix} 0 & I \\ -I & 0 \end{bmatrix} \begin{bmatrix} \frac{\partial H}{\partial q_m} \\ \frac{\partial H}{\partial p} \end{bmatrix} + \begin{bmatrix} 0 \\ B \end{bmatrix} u \right) = \left(\frac{\partial H}{\partial p}\right)^\top Bu =$$

$$p^\top M_r^{-1}(q_m)u = \dot{q}^\top u = y^\top u$$

The desired equilibrium is at $p = 0$, which is automatically incorporated into the Hamiltonian because kinetic energy is at a minimum when the momenta are zero, and $q_m = q_m^*$. Defining a new variable $\tilde{q}_m := q_m - q_m^*$ the desired Hamiltonian is proposed as:

$$H_d(q_m, p) := H(q_m, p) + \frac{1}{2}\|\tilde{q}_m\|_{K_I}^2$$

with K_I a constant gain matrix to be designed. This Hamiltonian has an extreme value at the equilibrium:

$$\frac{\partial H_d}{\partial x}\Big|_{\substack{p=0 \\ q_m=q_m^*}} = \begin{bmatrix} \frac{1}{2}\sum_{i=1}^{n} e_i p^\top \frac{\partial M_l^{-1}}{\partial q_{m_i}} p + K_I \tilde{q}_m \\ M_l^{-1} p \end{bmatrix}_{\substack{p=0 \\ q_m=q_m^*}} = \begin{bmatrix} 0 \\ 0 \end{bmatrix}$$

(with e_i a vector of zeros except for a 1 at the i'th position), and that extreme value is in fact, a minimum:

$$\frac{\partial^2 H_d}{\partial x^2}\Big|_{\substack{p=0 \\ q_m=q_m^*}} = \begin{bmatrix} K_I & 0 \\ 0 & M_l^{-1} \end{bmatrix} > 0$$

Now, the desired Hamiltonian can be rendered non-increasing by implementing the control law $u := -K_I \tilde{q}_m + v$:

$$\dot{H}_d = \dot{q}_m^\top u + \dot{q}_m^\top K_I \tilde{q}_m \qquad \Longrightarrow \qquad \dot{H}_d = 0 \quad \text{for } v = 0$$

This shows that the arm is stable with the desired Hamiltonian as a Lyapunov function. v can be used to inject damping ($v := -K_P \dot{q}_m$ with K_P a to be designed positive-definite matrix) and make the arm asymptotically stable:

$$\dot{H}_d = -\dot{q}_m^\top K_P \dot{q}_m \leq 0$$

Because the Hamiltonian's derivative is not negative definite, Barbashiin's theorem is used to prove asymptotic stability. All trajectories will converge to the largest invariant set in $\Omega := \left\{ q_m, p \in \mathbb{R}^{2n} \;\middle|\; \dot{H}_d = 0 \right\}$. If $\dot{H}_d = 0$ it follows that $\dot{q}_m = 0$ and therefore $p = 0$. With p a constant zero we find:

$$\dot{p} = -\frac{\partial H_d}{\partial q_m}\Big|_{p=0} - K_P M_l^{-1} p\Big|_{p=0} - K_I \tilde{q_m} = 0$$

$$\tilde{q}_m = 0 \qquad \Longrightarrow \qquad q_m = q_m^*$$

The only invariant set in Ω is therefore $(q_m, p) = (q_m^*, 0)$. This concludes the proof that the control law $u = -K_I \tilde{q}_m - K_P \dot{q}_m$ renders the equilibrium q_m^* asymptotically stable.

□

Results

The PI control in the rigid case performs similarly to the LQR control law. Convergence occurs in 2 to 4 seconds and overshoot is only slightly present in the simulated position of the first link. Again, a small steady-state error exists in the experimental results. See figure 4.1. As expected, this control law does not improve much on the results of the LQR. The rigid-joint system is similar enough to its linearized version to yield approximately the same results. Larger improvements might however be expected in the flexible case.

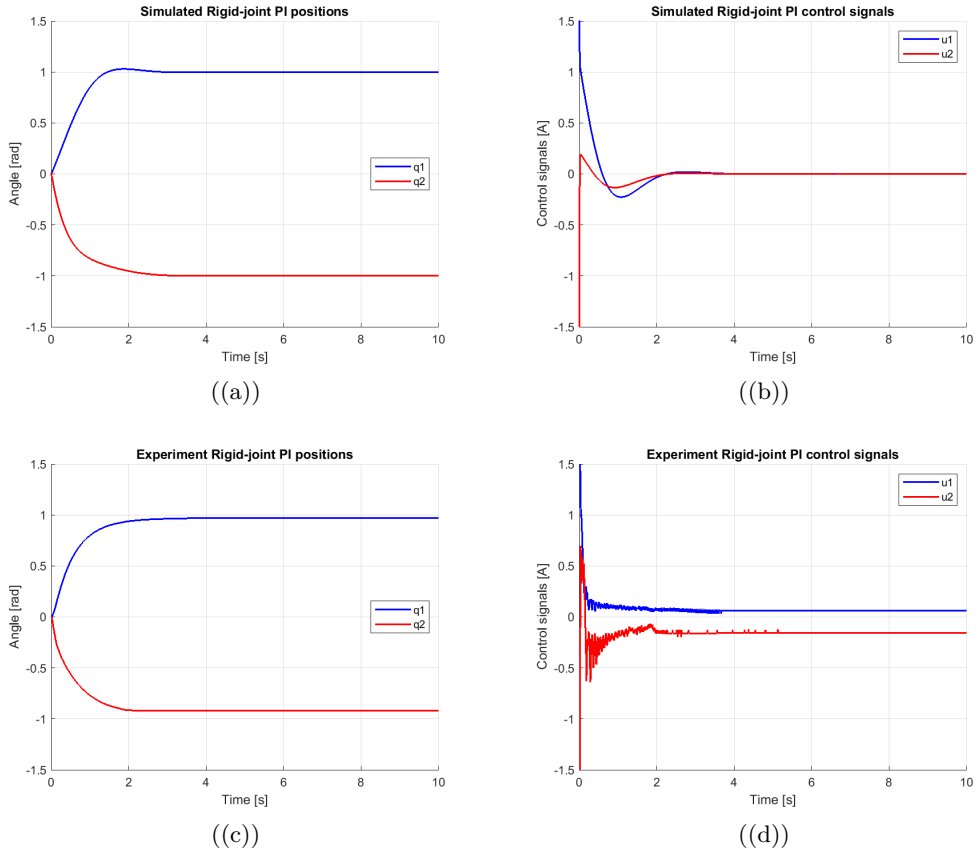

Figure 4.1: Simulated and experimental positions and control signals for PI control on rigid-joint arm

4.2 Flexible case

Proposition 4.2. *The control law* $u := -K_I\tilde{q}_m - K_P\dot{q}_m$ *renders the closed-loop system asymptotically stable.*

Proof. In the flexible case as in (3.2) with Hamiltonian (3.1) the desired equilibrium is at $p = 0$ and $q_l = q_m = q^*$ so that $x^* = (q_l^*, q_m^*, p_l^*, p_m^*)^\top = (q^*, q^*, 0, 0)^\top$. This time, in order to ease into upcoming sections, a more general formulation will be used. First, the passive output comes from finding the time-derivative of the current system's Hamiltonian, which is as follows:

$$\dot{H} = \begin{bmatrix} \left(\frac{\partial H}{\partial q}\right)^\top & \left(\frac{\partial H}{\partial p}\right)^\top \end{bmatrix} \begin{bmatrix} \dot{q} \\ \dot{p} \end{bmatrix} = p_m^\top M_m^{-1} u = \dot{q}_m^\top u$$

The passive output is identified as $y = \dot{q}_m$ and $\gamma := q_m$ is defined such that $\dot{\gamma} = y$. The energy function can now (in a general sense) be shaped as shown below:

$$H_d = H + \Theta(\gamma)$$

with Θ a to be determined function that has a minimum at the desired equilibrium. This means the derivative changes as follows:

$$\dot{H}_d = \dot{H} + y^\top \frac{\partial \Theta}{\partial \gamma}(\gamma) = y^\top u + y^\top \frac{\partial \Theta}{\partial \gamma}(\gamma) = y^\top \left(u + \frac{\partial \Theta}{\partial \gamma}(\gamma) \right)$$

Taking $u = -\frac{\partial \Theta}{\partial \gamma}(\gamma) - K_P y$ (with K_P a to be designed positive definite matrix) the Hamiltonian becomes non-increasing:

$$\dot{H}_d = -y^\top K_P y \leq 0$$

At this point the function Θ must be better specified. It must admit a minimum at the desired equilibrium and will loosely speaking act as a potential energy around this point. A variable is first defined as $\tilde{\gamma} = \gamma - \gamma^*$ where γ^* is the desired value for γ (in this case q^*). Now, Θ takes its final form:

$$\Theta(\gamma) = \frac{1}{2} \|\tilde{\gamma}\|_{K_I}^2 \qquad \text{so that} \qquad \frac{\partial \Theta}{\partial \gamma} = K_I \tilde{\gamma}$$

with K_I a to be designed positive definite matrix. Now to show that the new desired Hamiltonian indeed has a minimum at the desired equilibrium:

$$\frac{\partial H_d}{\partial x}\Big|_{x^*} = \begin{bmatrix} \frac{1}{2}\sum_{i=1}^{n} e_i p^\top \frac{\partial M_l^{-1}}{\partial q_i} p - K_s(q_m - q_l) \\ K_s(q_m - q_l) + K_I\tilde{\gamma} \\ p_l^\top M_l^{-1}(q_{l_2}) \\ p_m^\top M_m^{-1} \end{bmatrix}_* = 0$$

Furthermore, since the original Hamiltonian is positive definite and only the desired potential energy (those terms that only involve q) is changed, in this case the following inequalities are equivalent:

$$\frac{\partial^2 H_d}{\partial x^2}\Big|_* > 0 \quad \iff \quad \frac{\partial^2 V_d}{\partial x^2}\Big|_* > 0$$

with $V_d(q) = \frac{1}{2}\left\|q_m - q_l\right\|_{K_s}^2 + \frac{1}{2}\left\|\tilde{\gamma}\right\|_{K_I}^2$. Its Hessian:

$$\frac{\partial^2 V_d}{\partial x^2}\Big|_* = \begin{bmatrix} K_s & -K_s \\ -K_s & K_s + K_I \end{bmatrix}$$

Since $K_s = K_s^\top$ we can prove $\frac{\partial^2 V_d}{\partial x^2}$ is positive definite using Schür's complement:

$$\frac{\partial^2 V_d}{\partial x^2}\Big/ K_s = K_s + K_I - (-K_s)K_s^{-1}(-K_s) = K_s + K_I - K_s = K_I > 0$$

Now the solutions will converge to the largest invariant set in $\Omega = \left\{(q,p) \in \mathbb{R}^{2n} \;\middle|\; \dot{H}_d = 0\right\} = \left\{(q,p) \in \mathbb{R}^{2n} \;\middle|\; \tilde{\gamma} = \tilde{q}_m = 0\right\}$. This leads to $p_m = M_m\dot{q}_m = 0$ which in turn shows $\dot{p}_m = \ddot{p}_m = 0$, which finally gives:

$$\ddot{p}_m = K_s(\dot{q}_m - \dot{q}_l) + K_I\cancelto{0}{\ddot{q}_m} = 0$$

This shows $\dot{q}_l = 0$ which leads to $p_l = 0$. Then:

$$\dot{p}_l = K_s(q_m - q_l) = 0 \qquad \Longrightarrow \qquad q_l = q_m$$

From $\dot{p}_m = K_I\tilde{q}_m = 0$ the proof is now complete. □

Results

The flexible PI control outperforms the LQR. Convergence occurs in approximately 7 seconds in the simulations and 4 seconds in the experiments. It is possible that the friction causing the steady-state error plays a positive role in damping the oscillations. See figure 4.2. The steady-state error still exists, and from the control signals it can be seen that the control law is trying to correct them. The arms however will not move, which indicates that they are at a *sticking point*. This is further supported by the fact that the simulation (which does not consider the damping) does not feature a steady state error. A sticking point exists if the friction is higher when the arm is stationary. After overcoming the first friction to start moving the friction becomes slightly lower. An example of a friction model that can explain this is Stribeck friction [20].

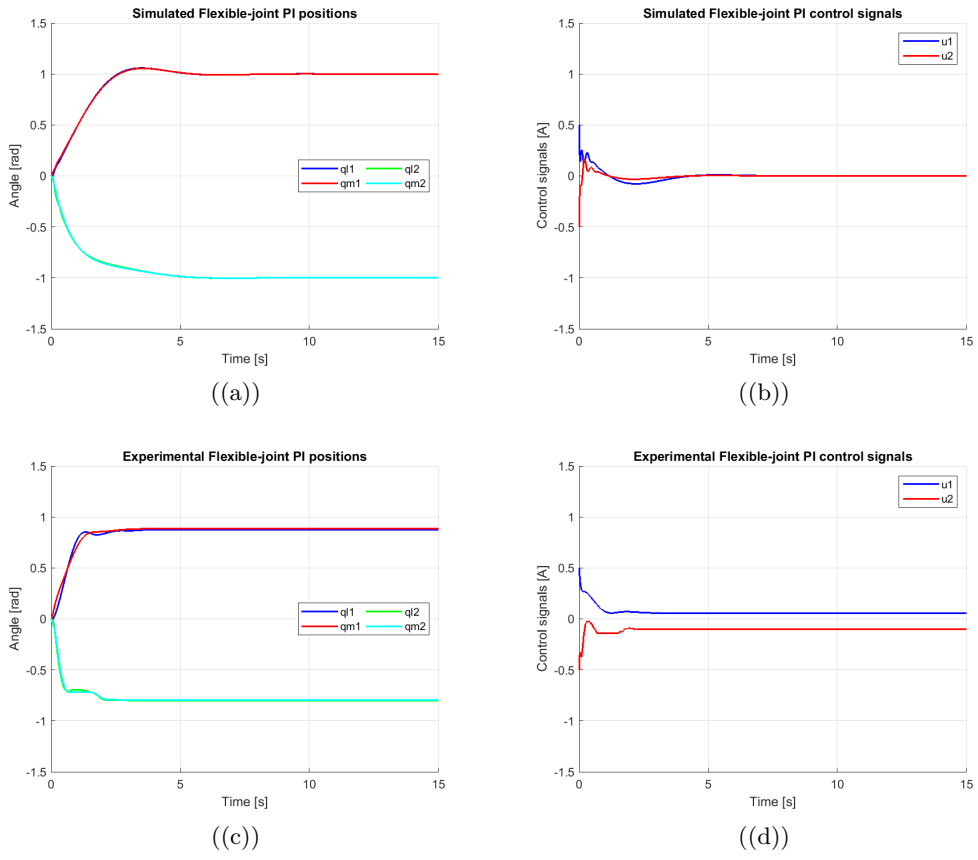

Figure 4.2: Simulated and experimental positions and control signals for PI control on flexible-joint arm

From these results it can be seen that the damping plays a considerable role in the performance of the proposed control laws. This damping however, has not been considered

in the analysis. The coming chapter will show why this is a problem.

Chapter 5

A case for considering natural damping

The flexible-joint control laws that were previously discussed performed better in theory than in practice. On the real arm, stabilizing the arm around the motor position takes a significant amount of time. This is partly because the damping is only injected in the motors, and oscillations in the link are then only damped because they propagate in the motors. In the real arm, friction in the motors and their actuation are enough to (under the previously discussed PI law) keep the motors fully stationary regardless of the links position and velocity. The movement of the link therefore, does not affect the motors and the oscillations in the links remain undamped. This is especially the case when the oscillations are small, and it takes a long time before such movement disappears. The links are then only damped by the natural damping, a limited effect.

During the experimentation phase, an intuitive solution for this problem was tried: to directly inject damping on the links, that is:

$$u := -K_I\tilde{q}_m - K_{P_1}\dot{q}_m - K_{P_2}\dot{q}_l = -K_I\tilde{q}_m - K_{P_1}M_m^{-1}p_m - K_{P_2}M_l^{-1}(q_l)p_l$$

The idea is that although the damping on the links is injected at the motors, it will propagate to quickly diminish the oscillations in the links. This control law proved to work exceptionally well under tuned versions of gain matrices K_I, K_{P_1} and K_{P_2} (all positive definite). In justifying this control laws the techniques that were used thus far seem lacking. In the classical PBC used in the following section use of any system state

apart from the passive output or its integral results in complicating cross-terms (picking up from (4.2):

$$\dot{H}_d = \dot{q}_m^\top \left(u + \frac{\partial \Phi}{\partial q_m}(q_m) \right) = -\dot{q}_m^\top K_{P_1} \dot{q}_m - \dot{q}_m^\top K_{P_2} \dot{q}_l \not\leq 0$$

The time-derivative of the Hamiltonian is clearly not negative semi-definite. In this case it is useful to see what inputs (and thus closed-loop dynamics) are possible whilst preserving a mechanical PH structure. IDA-PBC can show exactly this, take the dynamics in PH structure:

$$\dot{x} = f(x) + g(x)u = [J_d(x) - R_d(x)] \frac{\partial H_d}{\partial x}$$

The above equation formalizes that the open-loop system in combination with a control law u, should equate to a closed-loop system (without a free control law u) in mechanical PH form. To see what structures are possible the input is factored out by pre-multiplying both sides of the equation above by the full row-rank left-annihilator of $g(x)$ called $g^\perp$ (pronounced g-perp):

$$g^\perp \dot{x} \quad \Longrightarrow \quad g^\perp f = g^\perp [J_d(x) - R_d(x)] \frac{\partial H_d}{\partial x} \quad \Longrightarrow$$

$$g^\perp \left\{ [J(x) - R(x)] \frac{\partial H}{\partial x} - f(x) \right\} = 0 \tag{5.1}$$

In the case of the flexible link robot (and many other mechanical systems):

$$g(x) = \begin{bmatrix} 0 \\ B(x) \end{bmatrix} \quad \Longrightarrow \quad g^\perp = \begin{bmatrix} I & 0 \\ 0 & B^\perp(x) \end{bmatrix}$$

Since it is preferable to preserve the mechanical structure any desired Hamiltonian will have the following form: $H_d = V(q) + \frac{1}{2} p^\top M_d^{-1}(q) p$ and the final structure of the desired dynamics is as follows:

$$\begin{bmatrix} \dot{q} \\ \dot{p} \end{bmatrix} = \begin{bmatrix} 0 & M^{-1} M_d \\ -M^{-1} M_d & J_2 - D_d \end{bmatrix} \begin{bmatrix} \frac{\partial H_d}{\partial q} \\ M_d^{-1} p \end{bmatrix}$$

where the lower left part of the matrix is because the skew-symmetry is a requisite of a PH structure. $\dot{q}$ is equal to $M^{-1}(q)p$ as usual, from this it is clear that $\dot{q}$ cannot be

changed. The lower part of the conditions in (5.1) is:

$$B^{\perp}\left\{\frac{\partial H}{\partial q} - M_d M^{-1}\frac{\partial H_d}{\partial q} + \left[J_2 - D_d\right] M_d^{-1} p\right\} = 0$$

with:

$$B = \begin{bmatrix} 0 \\ I \end{bmatrix} \qquad \Longrightarrow \qquad B^{\perp} = \begin{bmatrix} I & 0 \\ 0 & 0 \end{bmatrix}$$

Solving this PDE called the matching condition will yield the possible structures and Hamiltonians. In this case however, since a control law has already been found, it is interesting to see if it is possible to retain the mechanical PH structure with that law. Therefore, the pre-multiplication with $B^{\perp}$ is reversed, the matching-condition now becomes:

$$-\frac{\partial H}{\partial q} + Bu = -M_d M^{-1}\frac{\partial H_d}{\partial q} + \left[J_2 - D_d\right] M_d^{-1} p$$

which can be split in two equations, one containing the potential energy, and one containing the kinetic energy. Equivalently, the matching condition is split up in one equation without the momenta p, and one containing p:

$$\begin{cases} -\frac{\partial V}{\partial q} + B\beta = -M_d M^{-1}\frac{\partial V_d}{\partial q} \\ -\frac{\partial T}{\partial q} + B\zeta = -M_d M^{-1}\frac{\partial T_d}{\partial q} + \big(J_2 - D_d\big) M_d^{-1} p \end{cases} \tag{5.2}$$

where ζ and β come from splitting up the control law similarly: $u = \beta(q) + \zeta(q,p)$. For the potential energy part, the first equation will show if the chosen control law alters the closed-loop mass-inertia matrix (if $M = M_d$ holds):

$$\begin{bmatrix} -K_s(q_l - q_m) \\ K_s(q_l - q_m) - K_I\tilde{q}_m \end{bmatrix} = M_d M^{-1} \begin{bmatrix} -K_s(q_l - q_m) \\ K_s(q_l - q_m) - K_I\tilde{q}_m \end{bmatrix}$$

This shows the mass-inertia matrix stays the same: $M_d = M$. Since $M = M_d$ implies T_d is equal to T the second equation now becomes:

$$B\zeta = \big(J_2 - D_d\big) M_d^{-1} p$$

$$\begin{bmatrix} 0 \\ -K_{P_1} - K_{P_2} \end{bmatrix} \dot{q} = \big(J_2 - D_d\big)\dot{q}$$

An option for J_2 and D_d is:

$$J_2 = \begin{bmatrix} 0 & \frac{1}{2}K_{P_2} \\ -\frac{1}{2}K_{P_2} & 0 \end{bmatrix} \qquad D_d = \begin{bmatrix} 0 & \frac{1}{2}K_{P_2} \\ \frac{1}{2}K_{P_2} & K_{P_1} \end{bmatrix}$$

These matrices however do not satisfy the requirements: $J_2 = -J_2^\top$ and $D_d = D_d^\top \geq 0$. The top-left part of D_d can never be non-zero (and therefore D_d cannot be positive semi-definite) when J_2 is skew-symmetric. From this it is apparent that the mechanical structure cannot be preserved under the proposed control law. Inspecting the eigenvalues of the linearized system shows that the proposed closed-loop system is even unstable, when the stability in the results from experimentation clearly indicate otherwise.

5.1 Considering the natural damping

The fact that the real system shows asymptotically stable behavior while analysis indicates instability suggests the problem might lie in the difference between these two environments. Although it could be possible that the system parameters are inaccurate, it is more likely that this difference is caused by a more radical distinction. In modelling the system, as is usual in literature, the damping is not considered. In doing so, the forms the control input can take whilst preserving mechanical PH structure and ensuring stability is strongly restricted. This can be shown when the damping in this case is considered (as linear damping with damping matrix D: a diagonal positive definite matrix) as in the following system:

$$\begin{bmatrix} \dot{q} \\ \dot{p} \end{bmatrix} = \begin{bmatrix} 0 & I \\ -I & -D \end{bmatrix} \begin{bmatrix} \frac{\partial H}{\partial q} \\ \frac{\partial H}{\partial p} \end{bmatrix} + \begin{bmatrix} 0 \\ B \end{bmatrix} u$$

The time-derivative of the desired Hamiltonian now shows the energy-dissipation caused by this damping:

$$\dot{H} = y^\top u - p^\top M^{-1} D M^{-1} p$$

Using the same calculations as in the previous section the equations in (5.2) look similar but with an important distinction:

$$\Sigma \begin{cases} -\frac{\partial V}{\partial q} + B\beta = -M_d M^{-1} \frac{\partial V_d}{\partial q} \\ -\frac{\partial T}{\partial q} + B\zeta = -M_d M^{-1} \frac{\partial T_d}{\partial q} + \big(J_2 - D_d\big) M_d^{-1} p + D M^{-1} p \end{cases}$$

The top equation did not change, the conclusion is therefore still $M_d = M$ which implies that also $T_d = T$. The lower equation rewrites to the following equality:

$$B\zeta = \big(J_2 - D_d + D\big) M_d^{-1} p$$

$$\begin{bmatrix} 0 & 0 \\ -K_{P_2} & -K_{P_1} \end{bmatrix} = J_2 - D_d + D = J_2 - D_d + \begin{bmatrix} D_l & 0 \\ 0 & D_m \end{bmatrix}$$

with J_2 and D_d free to choose as long as they satisfy the constraints for mechanical structures. A possible solution is then:

$$\begin{bmatrix} 0 & 0 \\ -K_{P_2} & -K_{P_1} \end{bmatrix} = \underbrace{\begin{bmatrix} 0 & \frac{1}{2}K_{P_2} \\ -\frac{1}{2}K_{P_2} & 0 \end{bmatrix}}_{J_2 = -J_2^\top} - \underbrace{\begin{bmatrix} D_l & \frac{1}{2}K_{P_2} \\ \frac{1}{2}K_{P_2} & D_m + K_{P_1} \end{bmatrix}}_{D_d = D_d^\top} + \begin{bmatrix} D_l & 0 \\ 0 & D_m \end{bmatrix}$$

$D_d = D_d^\top > 0$ if and only if (from Schür's complement):

$$K_{P_1} \geq \frac{1}{4} K_{P_2} D_l^{-1} K_{P_2} - D_m \tag{5.3}$$

If this condition is met, the mechanical port-Hamiltonian structure is preserved with a control law that initially seemed to violate these constraints. Now to prove the stability:

Proposition 5.1. *The control law* $u := -K_I \tilde{q}_m - K_{P_1} \dot{q}_m - K_{P_2} \dot{q}_l$ *asymptotically stabilizes the flexible-joint system.*

Proof. The following desired Hamiltonian is proposed:

$$H_d = H + \frac{1}{2} \left\| \tilde{q}_m \right\|_{K_I}^2$$

so that the H_d's derivative becomes:

$$\dot{H}_d = y^\top u - \begin{bmatrix} \dot{q}_l & \dot{q}_m \end{bmatrix} \begin{bmatrix} D_l & 0 \\ 0 & D_m \end{bmatrix} \begin{bmatrix} \dot{q}_l \\ \dot{q}_m \end{bmatrix}$$

Now substituting the proposed control law for u:

$$\dot{H}_d = - \begin{bmatrix} \dot{q}_l & \dot{q}_m \end{bmatrix} \underbrace{\begin{bmatrix} D_l & \frac{1}{2}K_{P_2} \\ \frac{1}{2}K_{P_2} & D_m + K_{P_1} \end{bmatrix}}_{D_d} \begin{bmatrix} \dot{q}_l \\ \dot{q}_m \end{bmatrix}$$

where D_d is the same matrix as encountered earlier and positive definite under condition (5.3). H_d now becomes a Lyapunov function showing that $\dot{q}_l = \dot{q}_m = 0$. Because $\dot{q}_l = 0$, $p_l = 0$ which leads to $\dot{p}_l = 0$. Then:

$$\dot{p}_l = K_s(q_m - q_l) = 0 \qquad \Longrightarrow \qquad q_l = q_m$$

Now:

$$\dot{p}_m = -K_I \tilde{q}_m = 0 \tag{5.4}$$

shows $\tilde{q} = 0$, completing the proof. □

Results

The PI control with damping on the links has excellent performance. Convergence occurs in 2 seconds. In this case, no steady-state error occurs. See figure 5.1. Is is likely that this is because the convergence occurs so fast that the arm does not settle at a sticking point before the set-point. The arm approaches the set-point at a high speed and stops relatively fast. The results are much better because of the added term. The oscillations in the links are damped immediately.

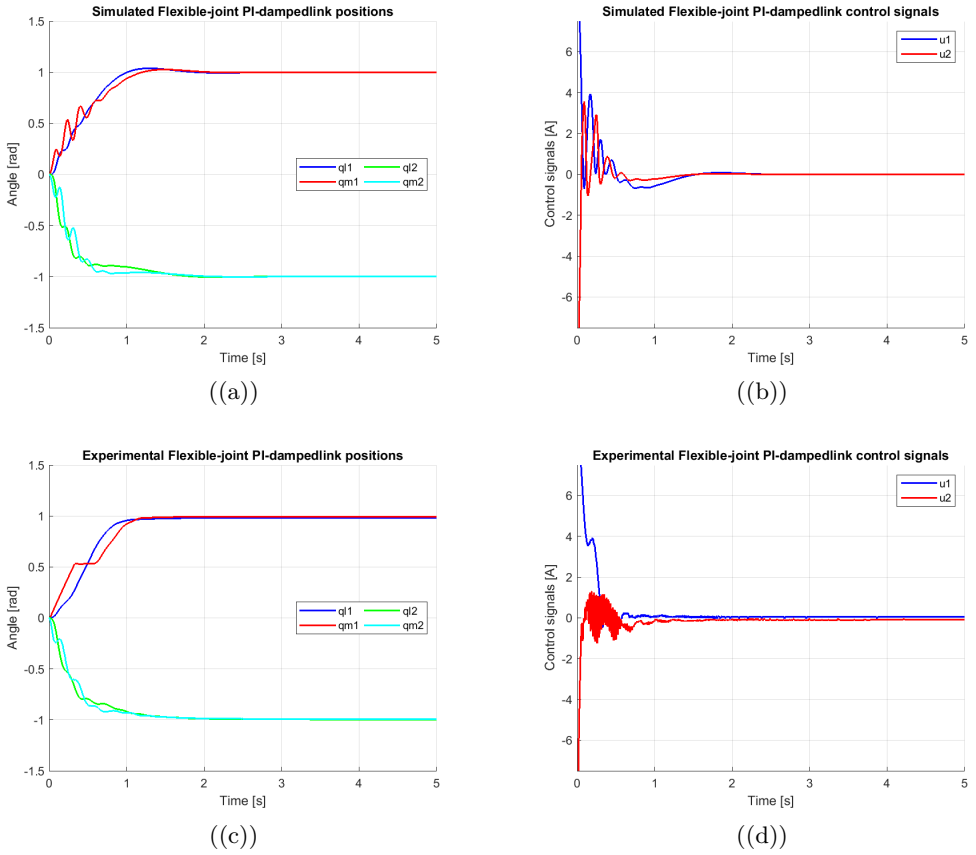

Figure 5.1: Simulated and experimental positions and control signals for PI control, with damping on the links, on flexible-joint arm

The performance is very significantly improved compared to the non-linear control law and even the normal PI-PBC control law. The control law however uses the velocity measurements of both the links and the motors and very high control signals are given, especially at time $t = 0$. The following chapters will check if the same results can be obtained whilst not using velocity measurements and saturating the signals.

Chapter 6

Saturated control without velocity measurements

As discussed in earlier sections, the availability and accuracy of velocity measurements is often limited. An explanation of a control that does not require these measurements, and additionally is saturated, is given in the coming sections, starting with the rigid case and then moving on to the flexible case. Damping will not be considered until explicitly mentioned.

6.1 Rigid case

Proposition 6.1. *The rigid system can be asymptotically stabilized by a naturally saturated control law* $u := \alpha \tanh z$

Proof. First, for the rigid case, some definitions are needed for the new control law. Since in the rigid case the link and motor positions are always the same, q_m will be used as angular position. The first defined variable, $\tilde{q}_m$, is a translation of q_m to the equilibrium. x_{c_i} is a new virtual state, the will be used as a virtual extension of the dynamics. z_i is a new variable that relates $\tilde{q}_m$ and the virtual states x_{c_i}.

$$\tilde{q}_{m_i} := q_{m_i} - q^*_{m_i}, \qquad z_i := \tilde{q}_{m_i} + x_{c_i}$$

The goal is to shape the Hamiltonian with an equilibrium at $x^* = (\tilde{q}_m, p, x_c)^\top = (0,0,0)^\top$ as follows:

$$H_d(q_m, p, x_c) = T(p, q_{m_2}) + \Phi_1(z_1) + \Phi_2(z_2) + \frac{1}{2}k_c x_{c_1}^2 + \frac{1}{2}k_c x_{c_2}^2$$

with $\Phi_i : \mathbb{R} \to \mathbb{R}$ a to be designed saturated function of the new state z, to help with constructing a saturated control law. The time-derivative of H_d is given as:

$$\dot{H}_d = y^\top u + \dot{\Phi}_1 + \dot{\Phi}_2 + \dot{x}_{c_1} k_c x_{c_1} + \dot{x}_{c_2} k_c x_{c_2} \tag{6.1}$$

Keeping in mind that because of the simple definition of z:

$$\frac{\partial z_i}{\partial q_{m_i}} = \frac{\partial z_i}{\partial x_{c_i}} \quad \Longrightarrow \quad \frac{\partial \Phi_i}{\partial x_{c_i}} = \frac{\partial \Phi_i}{\partial z_i}\frac{\partial z_i}{\partial x_{c_i}} = \frac{\partial \Phi_i}{\partial q_{m_i}}$$

and $y_i = q_{m_i}$, (6.1) can be rewritten as:

$$\dot{H}_d = y_1\Big(u_1 + \frac{\partial \Phi_1}{\partial x_{c_1}}\Big) + y_2\Big(u_2 + \frac{\partial \Phi_2}{\partial x_{c_2}}\Big) + \dot{x}_{c_1}\Big(k_c x_{c_1} + \frac{\partial \Phi_1}{\partial x_{c_1}}\Big) + \dot{x}_{c_2}\Big(k_c x_{c_2} + \frac{\partial \Phi_2}{\partial x_{c_2}}\Big) \tag{6.2}$$

The desired dynamics of the virtual states x_c and the inputs u now become clear:

$$\dot{x}_{c_i} := -r_c\Big(\frac{\partial H_d}{\partial x_{c_i}}\Big) = -r_c\Big(k_c x_{c_i} + \frac{\partial \Phi_i}{\partial x_{c_i}}\Big)$$

$$u_i := -\frac{\partial \Phi_i}{\partial x_{c_i}}$$

(6.2) now takes the following form:

$$\dot{H}_d = -r_c\Big(\frac{\partial H_d}{\partial x_{c_1}}\Big)^2 - r_c\Big(\frac{\partial H_d}{\partial x_{c_2}}\Big)^2 \leq 0$$

with $r_c > 0$ to be tuned gain constants. Now to show that x^* is an isolated minimum of H_d, H_d is split in a potential energy part and a kinetic energy part:

$$V_d(q_m, x_c) = \Phi_1(z_1) + \Phi_2(z_2) + \frac{1}{2}k_c x_{c_1}^2 + \frac{1}{2}k_c x_{c_2}^2$$
$$T_d(q_m, p) = \frac{1}{2}p^\top M^{-1}(q_{m_2})p$$

We find (provided that $\left(\frac{\partial \Phi}{\partial x}\right)_* = 0$, which will be discussed later):

$$\left(\frac{\partial H_d}{\partial x}\right)_* = \begin{bmatrix} \frac{\partial V_d}{\partial q_m} + \frac{\partial T_d}{\partial q_m} \\ M^{-1}(q_{m_2})p \\ \frac{\partial H_d}{\partial x_c} \end{bmatrix}_* = \begin{bmatrix} \mathbb{0}_{2x2} \\ \mathbb{0}_{2x2} \\ \mathbb{0}_{2x2} \end{bmatrix}$$

The Hessian of the desired Hamiltonian is (provided that $\left(\frac{\partial^2 \Phi}{\partial x^2}\right)_* = \alpha$, which will be discussed later):

$$\left(\frac{\partial^2 H_d}{\partial x^2}\right) = \begin{bmatrix} \frac{\partial^2 V_d}{\partial q_m^2} & \frac{\partial}{\partial p}\left(\frac{\partial T}{\partial q_m}\right) & \frac{\partial}{\partial x_c}\left(\frac{\partial V_d}{\partial q_m}\right) \\ \frac{\partial}{\partial q_m}\left(\frac{\partial T}{\partial p}\right) & M^{-1}(q_{m_2}) & 0 \\ \left(\frac{\partial}{\partial x_c}\left(\frac{\partial V_d}{\partial q_m}\right)\right)^\top & 0 & \frac{\partial^2 \Phi}{\partial x_c^2} + Ik_c \end{bmatrix}$$

which when evaluated at the equilibrium becomes:

$$\left(\frac{\partial^2 H_d}{\partial x^2}\right)_* = \begin{bmatrix} \alpha_1 & 0 & 0 & 0 & \alpha_1 & 0 \\ 0 & \alpha_2 & 0 & 0 & 0 & \alpha_2 \\ 0 & 0 & z_{11} & z_{12} & 0 & 0 \\ 0 & 0 & z_{21} & z_{22} & 0 & 0 \\ \alpha_1 & 0 & 0 & 0 & \alpha_1 + k_c & 0 \\ 0 & \alpha_2 & 0 & 0 & 0 & \alpha_2 + k_c \end{bmatrix} > 0$$

for:

$$M^{-1}(q_{m_2}) = \begin{bmatrix} z_{11} & z_{12} \\ z_{21} & z_{22} \end{bmatrix}$$

showing that the equilibrium x^* is an isolated minimum of H_d. Since $\dot{H}_d \leq 0$, or non-increasing, the following follows from the fundamental law of calculus:

$$\int_0^t \dot{H}_d(\tau)d\tau = H_d(t) - H_d(0) \leq 0$$

$$\lim_{t\to\infty} H_d(t) \leq H_d(0) < \infty \tag{6.3}$$

Because H_d is bounded from below, non-increasing and radially unbounded (requiring that Φ is radially unbounded) it can be concluded that its variables q_m, p, x_c are bounded. The derivatives of these values are also bounded. Since $\dot{H}_d$ is negative semi-definite, all

solutions of the states converge to the following set:

$$\Omega := \{\, (q_m, p, x_c) \in \mathbb{R}^6 \mid \dot{H}_d = 0 \,\}$$

In this set the following is already apparent:

$$\dot{H}_d = 0 \implies \begin{cases} \dot{x}_c = 0 \\ k_c x_c = -\frac{\partial \Phi_i}{\partial x_c} \end{cases}$$

To induce more about what is happening within Ω the following auxiliary function is defined:

$$\mathcal{U}_1 := -x_{c_1} p_1 \implies \dot{\mathcal{U}}_1 = -\dot{x}_{c_1}\overset{0}{\cancel{p_1}} - x_{c_1}\dot{p}_1 = -x_{c_1} u_1 = x_{c_1}\frac{\partial \Phi_1}{\partial x_{c_1}} = -k_c x_{c_1}^2 \leq 0 \qquad (6.4)$$

Since the variables x_{c_1} and p_1 are bounded, $\mathcal{U}_1$ is bounded from below. $\dot{\mathcal{U}}$ is negative semi-definite and $\ddot{\mathcal{U}}_2 = -k_c \dot{x}_{c_1}\overset{0}{\cancel{x_{c_1}}}$ is finite. This means that (invoking corollary 2.10 of Barbalat's lemma) $\dot{\mathcal{U}}_1 \to 0$ as $t \to \infty$, implying that $x_{c_1} \to 0$ as $t \to \infty$ as well. This sets off the following line of reasoning:

$$x_{c_1} \to 0 \quad \implies \quad \frac{\partial \Phi_1}{\partial x_{c_1}} \to 0 \quad \implies \quad z_1 \to 0 \quad \implies \quad \tilde{q}_{m_1} \to 0 \quad \implies \quad q_{m_1} \to q^*_{m_1}$$

It can already be seen (for the convergence of q_{m_2}) that:

$$q_{m_1} \to q^*_{m_1} \quad \implies \quad \frac{\partial T}{\partial q_{m_2}} = (\dot{q}_{m_1} + \dot{q}_{m_2})\overset{0}{\cancel{\dot{q}_{m_1}}} b \sin q_{m_2} \to 0$$

A second auxiliary function is now defined:

$$\mathcal{U}_2 := -x_{c_2} p_2 \implies \dot{\mathcal{U}}_2 = -\dot{x}_{c_2}\overset{0}{\cancel{p_2}} - x_{c_2}\dot{p}_2 = -x_{c_2}\Big(u_2 + \overset{0}{\cancel{\frac{\partial T}{\partial q_{m_2}}}}\Big) = x_{c_2}\frac{\partial \Phi_2}{\partial x_{c_2}} = -k_c x_{c_2}^2 \leq 0$$

Having arrived at the same point as in (6.4) the proof of stability is now close:

$$\dot{\mathcal{U}}_2 \to 0 \quad \implies \quad x_{c_2} \to 0 \quad \implies \quad \frac{\partial \Phi_2}{\partial x_{c_2}} \to 0 \quad \implies$$

$$z_2 \to 0 \quad \implies \quad \tilde{q}_{m_2} \to 0 \quad \implies \quad q_{m_2} \to q^*_{m_2}$$

The only thing that is now left is to choose Φ such that $\left(\frac{\partial \Phi}{\partial x}\right)_* = 0$, $\left(\frac{\partial^2 \Phi}{\partial x^2}\right)_* = \alpha$ and Φ is radially unbounded. This brings the interesting possibility to saturate the control input. If Φ is chosen such that $\frac{\partial \Phi}{\partial x}$ is the hyperbolic tangent, the norm of the control signal will never exceed a certain value (see figure 6.1), since u only depends on this $\frac{\partial \Phi}{\partial x}$. This leads to the following definition of Φ for $i = 1, 2$:

$$\begin{aligned} \Phi_i &:= \alpha_i \ln \cosh z_i \\ \frac{\partial \Phi_i}{\partial x} &= \alpha_i \tanh z_i \\ \frac{\partial^2 \Phi_i}{\partial x^2} &= \alpha_i \operatorname{sech} z_i \end{aligned}$$

with $\alpha_i > 0$ the saturation limit which the control signal will never exceed. This satisfies the assumptions that were left to discuss:

1. $\Phi_i(z_i) > 0 \quad \forall z_i \neq 0, \qquad \Phi_i(z_i^*) = 0$
2. $\frac{\partial \Phi_i}{\partial x}(z_i^*) = 0$
3. $\frac{\partial^2 \Phi_i}{\partial x^2}(z_i^*) = \alpha_i$
4. $\lim\limits_{|q, x_c| \to \infty} \alpha_i \ln \cosh z_i = \infty$

with $z^* = \tilde{q}_m^* + x_c^* = 0$.

□

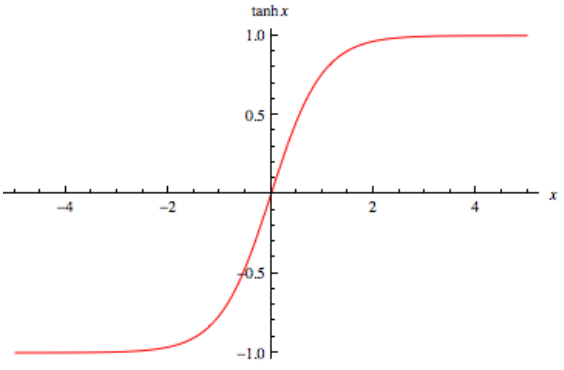

Figure 6.1: The hyperbolic tangent $\alpha \tanh x$ with $\alpha = 1$

Results

The saturated control performs well on the rigid set-up. Performance is again approximately equal to the LQR as convergence occurs in around 2 seconds. The experiment produces a negligible steady-state error. See figure 6.2.

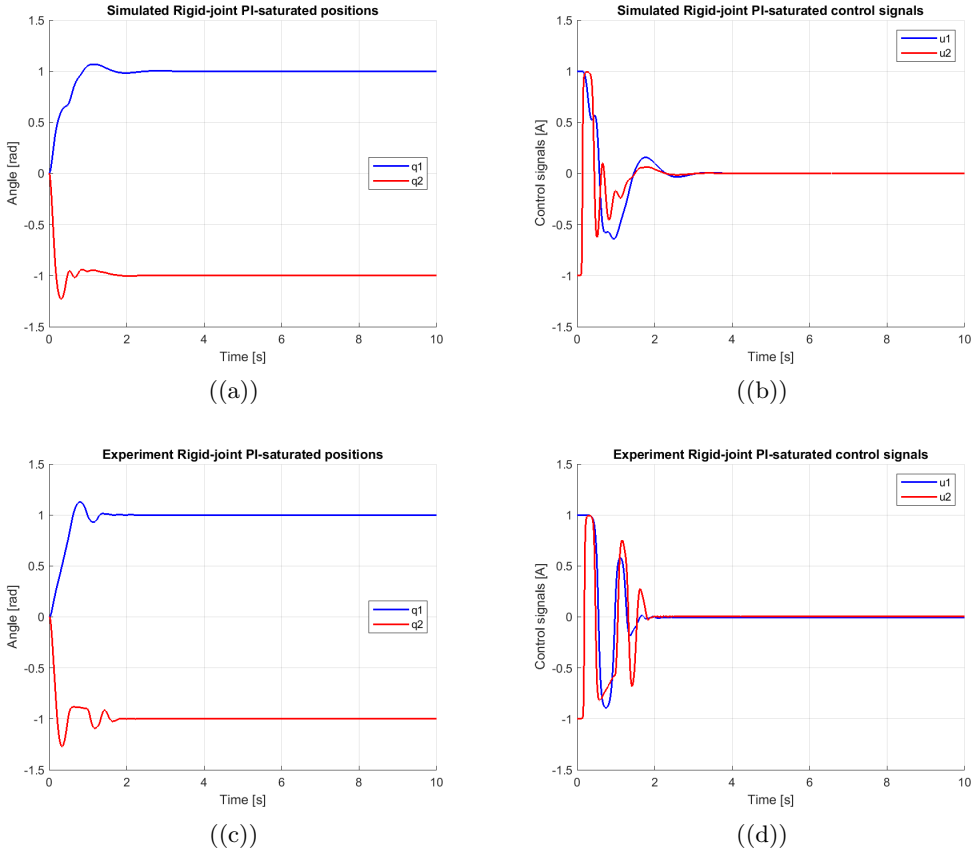

Figure 6.2: Simulated and experimental positions and control signals for saturated control on rigid-joint arm

6.2 Flexible case

Proposition 6.2. *The rigid system can be asymptotically stabilized by a naturally saturated control law* $u := \alpha \tanh z$

Proof. For the flexible case the system as in (3.2) is considered:

$$\begin{bmatrix} \dot{q} \\ \dot{p} \end{bmatrix} = \begin{bmatrix} 0 & I \\ -I & 0 \end{bmatrix} \begin{bmatrix} K_s(q_m - q_l) + \frac{\partial T}{\partial q} \\ M^{-1}(q_2)p \end{bmatrix} + \begin{bmatrix} 0 \\ G \end{bmatrix} u, \qquad G = \begin{bmatrix} \mathbb{0}_{2\times 2} \\ I_{2\times 2} \end{bmatrix}$$

with:

$$M(q_{l_2}) = \begin{bmatrix} M_l(q_{l_2}) & 0 \\ 0 & M_m \end{bmatrix}, \qquad T = \frac{1}{2} p_l^\top M_l^{-1}(q_{l_2}) p_l + \frac{1}{2} p_m^\top M_m^{-1} p_m$$

The passive output is identified as follows:

$$H = \frac{1}{2}(q_m - q_l)^\top K_s (q_m - q_l) + T(q_l, p_l, p_m)$$

$$\dot{H} = \dot{q}_m^\top u, \qquad y = \dot{q}_m, \qquad \gamma = q_m$$

Now defining:

$$z := \tilde{q}_m + x_c \ , \qquad z, x_c \in \mathbb{R}^2$$

and:

$$H_d := H + \Phi_1(z_1) + \Phi_2(z_2) + \frac{1}{2}\|x_{c_1}\|^2_{K_{c_1}} + \frac{1}{2}\|x_{c_2}\|^2_{K_{c_2}}$$

$$\dot{H}_d = \dot{H} + \dot{\Phi}_1 + \dot{\Phi}_2 + \dot{x}_{c_1} k_{c_1} x_{c_1} + \dot{x}_{c_2} k_{c_2} x_{c_2} \tag{6.5}$$

Noting that because of the definition of z:

$$\frac{\partial \Phi_i}{\partial q_i} = \frac{\partial \Phi_i}{\partial x_{c_i}}$$

(6.5) can be rewritten as follows:

$$\begin{aligned} \dot{H}_d = q_{m_1}^\top \Big(u_1 + \frac{\partial \Phi_1}{\partial q_{m_1}} \Big) + q_{m_2}^\top \Big(u_2 + \frac{\partial \Phi_2}{\partial q_{m_2}} \Big) + \\ \dot{x}_{c_1} \Big(k_{c_1} x_{c_1} + \frac{\partial \Phi_1}{\partial q_{m_1}} \Big) + \dot{x}_{c_2} \Big(k_{c_2} x_{c_2} + \frac{\partial \Phi_2}{\partial q_{m_2}} \Big) \end{aligned} \tag{6.6}$$

Defining the following:

$$u_1 := -\frac{\partial \Phi_1}{\partial q_{m_1}} \qquad\qquad u_2 := -\frac{\partial \Phi_2}{\partial q_{m_2}}$$

$$\dot{x}_{c_1} := -R_{c_1}\frac{\partial H_d}{\partial x_{c_1}} \qquad\qquad \dot{x}_{c_2} := -R_{c_2}\frac{\partial H_d}{\partial x_{c_2}}$$

with R_c free positive definite diagonal matrices, (6.6) now becomes:

$$\dot{H}_d = -\Big\| \underbrace{k_{c_1}x_{c_1} + \frac{\partial \Phi_1}{\partial x_{c_1}}}_{\frac{\partial H_e}{\partial x_{c_1}}} \Big\|^2_{R_{c_1}} - \Big\| \underbrace{k_{c_2}x_{c_2} + \frac{\partial \Phi_2}{\partial x_{c_2}}}_{\frac{\partial H_e}{\partial x_{c_2}}} \Big\|^2_{R_{c_2}} \leq 0$$

The fundamental law of calculus yields the following:

$$\int_0^t \dot{H}_d \, \mathrm{d}t \leq \int_0^t 0 \, \mathrm{d}t \implies H_d(t) - H_d(0) \leq 0 \implies 0 \leq H_d(t) \leq H_d(0) < \infty$$

Because H_d is bounded from below, non-increasing and radially unbounded (requiring that Φ is radially unbounded) it can be concluded that its variables q, p, x_c are bounded. The derivatives of these values are also bounded. The solutions converge to the set $\Omega := \big\{(q,p,x_c) \in \mathbb{R}^{10} \;\big|\; \dot{H}_d = 0\big\}$, in which the following is known:

$$\Omega \implies \begin{cases} \dot{x}_{c_i} = 0 & \forall i \in \{1,2\} \\ x_{c_i}k_{c_i} = -\frac{\partial \Phi_i}{\partial x_{c_i}} & \forall i \in \{1,2\} \end{cases}$$

The following auxiliary function is defined:

$$\mathcal{U}_1 := -x_{c_1}\big(p_{m_1} + p_{l_1}\big)$$

such that:

$$\dot{\mathcal{U}}_1 = -\cancelto{0}{\dot{x}_{c_1}}\big(p_{m_1} + p_{l_1}\big) - x_{c_1}\big(\dot{p}_{m_1} + \dot{p}_{l_1}\big) = -x_{c_1}u_1 = x_{c_1}\frac{\partial \Phi_1}{\partial x_{c_1}} = -k_{c_1}x_{c_1}^2 \leq 0$$

Using corollary 2.10 of Barbalat with the same arguments as (6.4) it can be seen that $\mathcal{U}_1 \to 0$ as $t \to \infty$ and therefore: $x_{c_1} \to 0$ as $t \to \infty$. As $x_{c_1} \to 0 \implies \frac{\partial \Phi_1}{\partial x_{c_1}} \to 0 \implies z_1 \to 0 \implies \tilde{q}_{m_1} \to 0 \implies \dot{q}_{m_1} \to 0 \implies p_{m_1} \to 0 \implies \dot{p}_{m_1} \to -K_1(q_{m_1} - q_{l_1}) + \cancelto{0}{\frac{\partial \Phi_1}{\partial q_{m_1}}} \to 0 \implies q_{m_1} \to q_{l_1} \implies \dot{q}_{l_1} \to 0$

A second auxiliary function is now defined as:

$$\mathcal{U}_2 := -x_{c_2}\big(p_{m_2} + p_{l_2}\big)$$

$$\dot{\mathcal{U}}_2 = -\cancelto{0}{\dot{x}_{c_2}}(p_{m_2} + p_{l_2}) - x_{c_2}(\dot{p}_{m_2} + \dot{p}_{l_2}) = -x_{c_2}\Big(u_1 - \cancelto{0}{\frac{\partial T}{\partial q_{l_2}}}\Big) = x_{c_2}\frac{\partial \Phi_2}{\partial x_{c_2}} = -k_{c_2}x_{c_2}^2 \leq 0$$

Using Barbalat again using similar steps as for link 1 it can be seen that $\mathcal{U}_2 \to 0$ as $t \to \infty$ and therefore: $x_{c_2} \to 0$ as $t \to \infty$. As $x_{c_2} \to 0 \implies \frac{\partial \Phi_2}{\partial x_{c_2}} \to 0 \implies z_2 \to 0 \implies \tilde{q}_{m_2} \to 0 \implies \dot{q}_{m_2} \to 0 \implies p_{m_2} \to 0 \implies \dot{p}_{m_2} \to -K_2(q_{m_2} - q_{l_2}) + \cancelto{0}{\frac{\partial \Phi_2}{\partial q_{m_2}}} \to 0 \implies q_{m_2} \to q_{l_2} \implies \dot{q}_{l_2} \to 0$

This completes the proof that x^* is now an asymptotically stable point of the closed loop system. □

Results

The controller converges similarly to the flexible-case LQR, as convergence takes approximately 7 seconds. A large steady-state error exists in the experimental case. Link 1 oscillates around the motor for considerable time in the experiments. See figure 6.3. The performance is worse than the performance of the enhanced PI law. The control signal is now however saturated and the velocity measurements are no longer used.

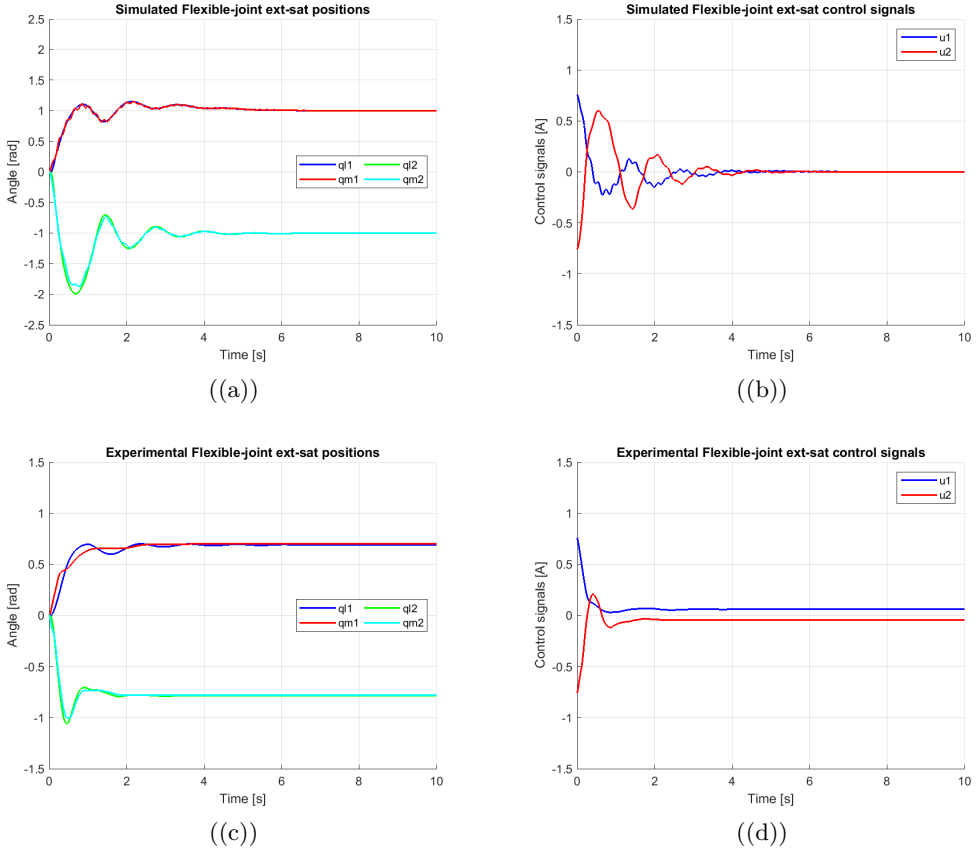

Figure 6.3: Simulated and experimental positions and control signals for saturated control on flexible-joint arm

The trade-off between information about the velocity and saturation on the one side, and performance on the other could have been expected. The results do indeed suffer when not all states can be used for the feedback. The damage is not too large, and further tweaks can improve the performance further.

6.3 Flexible case with damping on the links

Proposition 6.3. *The control law* $u := -\frac{\partial \Phi_m}{\partial q_m} - \alpha \frac{\partial \Phi_l}{\partial q_l}$ *can asymptotically stabilize the flexible-joint system.*

Proof. In order to inject damping based on the velocity in the links, the natural damping will be considered in this case. This means the system under consideration is the system as in (5.1) such that:

$$\dot{H} = \dot{q}_m^\top u - p^\top M^{-1} D M^{-1} p$$

Defining:

$$z_m := \tilde{q}_m + x_m \qquad\qquad z_l := \tilde{q}_l + x_l$$

the desired Hamiltonian can be formulated as follows:

$$H_d := H + \frac{1}{2} \|x_m\|_{K_m}^2 + \Phi_m(z_m) + \Phi_l(z_l) \tag{6.7}$$

and its derivative is given as:

$$\begin{aligned} \dot{H}_d = -\begin{bmatrix} \dot{q}_l^\top & \dot{q}_m^\top \end{bmatrix} \begin{bmatrix} D_l & 0 \\ 0 & D_m \end{bmatrix} \begin{bmatrix} \dot{q}_l \\ \dot{q}_m \end{bmatrix} + \dot{q}_m^\top u + \dot{q}_m^\top \frac{\partial \Phi_m}{\partial q_m} \\ + \dot{x}_m \left(\frac{\partial \Phi_m}{\partial q_m} + K_c x_m \right) + \dot{q}_l^\top \frac{\partial \Phi_l}{\partial q_l} + \dot{x}_l^\top \frac{\partial \Phi_l}{\partial q_l} \end{aligned} \tag{6.8}$$

When the following control input and virtual state dynamics are chosen:

$$\dot{x}_m := -R_m \left(\frac{\partial \Phi_m}{\partial q_m} + K_c x_m \right) \qquad\qquad \dot{x}_l := -R_l \frac{\partial \Phi_l}{\partial q_m} \tag{6.9}$$

$$u := -\frac{\partial \Phi_m}{\partial q_m} - \alpha \frac{\partial \Phi_l}{\partial q_l}$$

with R_m, R_l, K_c positive definite gain matrices to be designed, equation (6.8) rewrites as follows:

$$\dot{H}_d = -\frac{1}{2} \left\| \frac{\partial \Phi_m}{\partial q_m} + K_c x_m \right\|_{R_m}^2 - \begin{bmatrix} \dot{q}_l^\top & \dot{q}_m^\top & \frac{\partial \Phi_l}{\partial q_l}^\top \end{bmatrix} \underbrace{\begin{bmatrix} D_l & 0 & -I \\ 0 & D_m & \alpha \\ 0 & 0 & R_l \end{bmatrix}}_{= R_{mat}} \begin{bmatrix} \dot{q}_l \\ \dot{q}_m \\ \frac{\partial \Phi_l}{\partial q_l} \end{bmatrix}$$

Since $D_l, R_l > 0$, R_{mat} is positive definite when the following condition holds:

$$D_l - \begin{bmatrix} 0 & \frac{1}{2}I \end{bmatrix} \begin{bmatrix} D_m & \frac{1}{2}\alpha \\ \frac{1}{2}\alpha & R_l \end{bmatrix}^{-1} \begin{bmatrix} 0 \\ \frac{1}{2}I \end{bmatrix} \geq 0$$

$$\begin{bmatrix} D_m & \frac{1}{2}\alpha \\ \frac{1}{2}\alpha & R_l \end{bmatrix} - \begin{bmatrix} 0 \\ \frac{1}{2}I \end{bmatrix} D_l^{-1} \begin{bmatrix} 0 & \frac{1}{2}I \end{bmatrix} = \begin{bmatrix} D_m & \frac{1}{2}\alpha \\ \frac{1}{2}\alpha & R_l - \frac{1}{4}D_l^{-1} \end{bmatrix} \geq 0$$

Using Schür's complement this is equivalent to:

$$R_l - \frac{1}{4}D_l^{-1} - \frac{1}{4}\alpha^2 D_m^{-1} \geq 0 \tag{6.10}$$

This only works when:

$$\begin{bmatrix} D_m & \frac{1}{2}\alpha \\ \frac{1}{2}\alpha & R_l \end{bmatrix}$$

is invertible, which it is when it is positive definite. From applying Schür's complement again another bound on R_l is found:

$$R_l - \frac{1}{4}\alpha^2 D_m^{-1} > 0$$

this bound is however not as tight and therefore satisfied automatically if (6.10) is satisfied. Since R_l is free to design H_d can always be rendered non-increasing and all solutions will converge to $\Omega := \left\{(q, p, x_l, x_m) \in \mathbb{R}^{12} \;\middle|\; \dot{H}_d = 0\right\}$. In this set the following is known:

$$\Omega \implies \begin{cases} K_c x_m = -\frac{\partial \Phi_m}{\partial x_m} \implies \dot{x}_m = 0 \\ \dot{q}_l, \dot{q}_m = 0 \implies p_l, p_m = 0 \implies \dot{p}_l, \dot{p}_m = 0 \\ \frac{\partial \Phi_l}{\partial q_l} = 0 \implies z_l = 0 \implies \tilde{q}_l = -x_l \end{cases}$$

Then since:

$$\dot{p}_l + \dot{p}_m = -\frac{\partial \Phi_m}{\partial q_m} = 0 \implies x_m = 0 \implies q_m = q_m^*$$

$$\dot{p}_l = \frac{\partial V}{\partial q_l} = 0 \implies q_l = q_m = 0$$

this completes the proof that $(q, p, x_l, x_m) = (\tilde{q}, 0, 0, 0)$ is asymptotically stable. □

One downside of this control law is that the PH structure of the closed loop system cannot be preserved under this control law. Since only the motors are actuated the open loop $\dot{p}_l$ does not depend on the input u. This means that the closed loop $\dot{p}_l$ must be exactly equal to the open loop $\dot{p}_l$. These however do not match, comparing the two dynamics:

$$\dot{p}_{l_{OL}} = -\frac{\partial H}{\partial q_l} - D_l \frac{\partial H}{\partial p_l} = -\frac{\partial T}{\partial q_l} - K_s(q_l - q_m) - D_l M^{-1} p_l$$
$$\dot{p}_{l_{CL}} = -\frac{\partial H_d}{\partial q_l} - D_l \frac{\partial H_d}{\partial p_l} = -\frac{\partial H}{\partial q_l} - D_l \frac{\partial H}{\partial p_l} - \frac{\partial \Phi_l}{\partial q_l}$$

Results

Convergence occurs in around 6 seconds. A steady-state error exists but it is smaller than the saturated control without damping on the links. The control signals are saturated at 1.2 and -1.2. See figure 6.4. The effects of adding damping in the links is not as large as in the normal PI control. There are less oscillations but they still exist. The steady state error is also still present, this problem will be tackled in the next section.

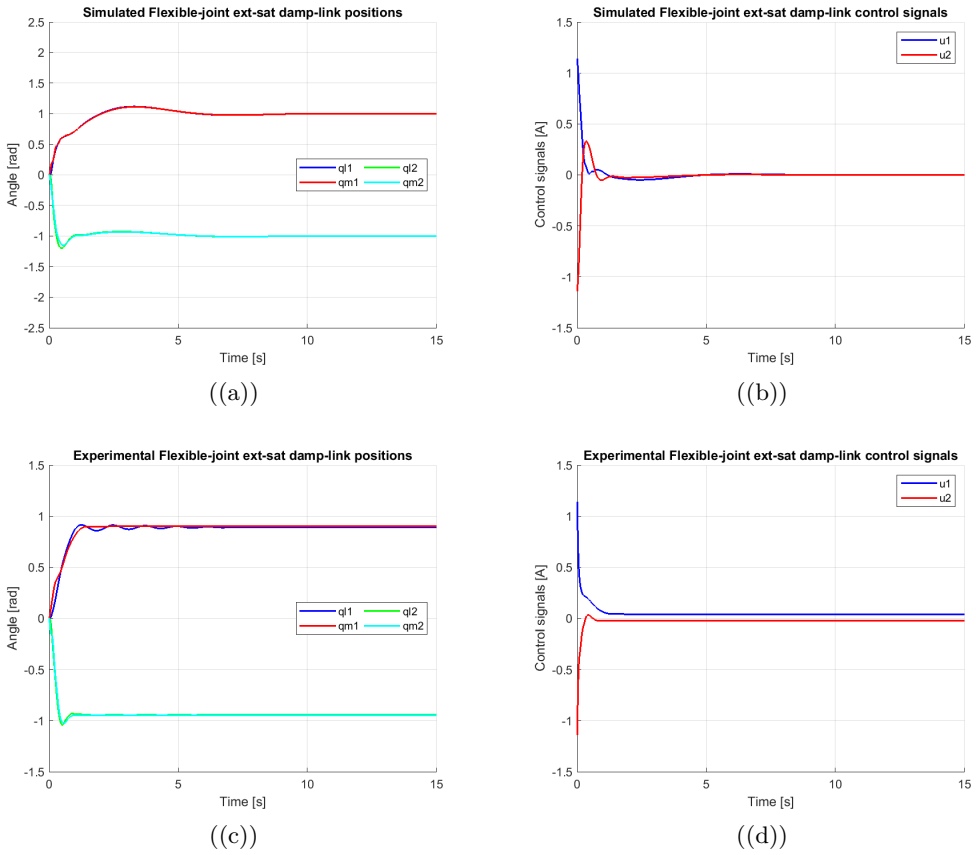

Figure 6.4: Simulated and experimental positions and control signals for saturated control, with damping on the links, on flexible-joint arm

6.4 Integral term on position

Tests in the experimental set-up revealed the existence of stead-state errors that were not present in the simulations. Although the current control has a proportional and integral term, these terms are named with respect to the passive output $\dot{q}_m$. The integral term acts on q_m or motor positions and does therefore not correct any steady-state errors. An

extra integral action on the position can prevent these errors. A new virtual state σ will be introduced for this purpose. However, it is more convenient to couple $\dot{\sigma}$ to the virtual state x_m (which is strongly related to q_m) than to q_m directly. This is because coupling σ to the x_m makes it easier to preserve the PH structure (it can easily be coupled to $\frac{\partial H}{\partial x_m}$).

Proposition 6.4. *The control law* $u := -\frac{\partial \Phi_m}{\partial q_m} - \alpha \frac{\partial \Phi_l}{\partial q_l} + \beta \frac{\partial \Phi_\sigma}{\partial \sigma}$ *together with virtual state dynamics* $\dot{\sigma} := \gamma \left(\frac{\partial \Phi_m}{\partial q_m} + K_c x_m \right) - R_\sigma \frac{\partial \Phi_\sigma}{\partial \sigma}$ *can asymptotically stabilize the flexible-joint system.*

Proof. First the desired Hamiltonian extends H_d from the previous case (6.7):

$$H_\sigma = H_d + \Phi_\sigma$$

with Φ_σ such that $\frac{\partial \Phi_\sigma}{\partial x}$ is some form of the hyperbolic tangent. Taking $\dot{x}_l, \dot{x}_m$ as in (6.9), and u and $\dot{\sigma}$:

$$u := -\frac{\partial \Phi_m}{\partial q_m} - \alpha \frac{\partial \Phi_l}{\partial q_l} + \beta \frac{\partial \Phi_\sigma}{\partial \sigma} \qquad \dot{\sigma} := \gamma \left(\frac{\partial \Phi_m}{\partial q_m} + K_c x_m \right) - R_\sigma \frac{\partial \Phi_\sigma}{\partial \sigma}$$

with K_c, R_σ positive definite gain matrices to be designed, the entire closed loop dynamics become:

$$\begin{bmatrix} \dot{q}_l \\ \dot{q}_m \\ \dot{p}_l \\ \dot{p}_m \\ \dot{x}_l \\ \dot{x}_m \\ \dot{\sigma} \end{bmatrix} = \begin{bmatrix} 0 & 0 & I & 0 & 0 & 0 & 0 \\ 0 & 0 & 0 & I & 0 & 0 & 0 \\ -I & 0 & -D_l & 0 & 0 & 0 & 0 \\ 0 & -I & 0 & -D_m & -\alpha & -I & \beta \\ 0 & 0 & 0 & 0 & -R_l & 0 & 0 \\ 0 & 0 & 0 & 0 & 0 & -R_m & 0 \\ 0 & 0 & 0 & 0 & 0 & \gamma & -R_\sigma \end{bmatrix} \frac{\partial H_\sigma}{\partial x}$$

The Hamiltonian's derivative is as follows:

$$\dot{H}_\sigma = \dot{H}_d + \dot{q}_m^\top \beta \frac{\partial \Phi_\sigma}{\partial \sigma} + \dot{\sigma}^\top \frac{\partial \Phi_\sigma}{\partial \sigma} = \dot{H}_d + \dot{q}_m^\top \beta \frac{\partial \Phi_\sigma}{\partial \sigma} + \left(\frac{\partial \Phi_l}{\partial q_l} - R_\sigma \frac{\partial \Phi_\sigma}{\partial \sigma} \right)^\top \frac{\partial \Phi_\sigma}{\partial \sigma}$$

$$= -\Psi^\top \underbrace{\begin{bmatrix} R_m & -\frac{1}{2}\gamma & 0 & 0 & 0 \\ -\frac{1}{2}\gamma & R_\sigma & 0 & \frac{1}{2}\beta & 0 \\ 0 & 0 & D_l & 0 & -\frac{1}{2}I \\ 0 & \frac{1}{2}\beta & 0 & D_m & \frac{1}{2}\alpha \\ 0 & 0 & -\frac{1}{2}I & \frac{1}{2}\alpha & R_l \end{bmatrix}}_{=R_{mat}} \underbrace{\begin{bmatrix} \frac{\partial \Phi_m}{\partial q_m} + K_c x_m \\ \frac{\partial \Phi_\sigma}{\partial \sigma} \\ \dot{q}_l \\ \dot{q}_m \\ \frac{\partial \Phi_l}{\partial q_l} \end{bmatrix}}_{=\Psi} < 0$$

in R_{mat} from the last paragraph is shown that the lower 3×3 blocks part of the matrix is positive definite when $R_l - \frac{1}{4}D_l^{-1} - \frac{1}{4}\alpha^2 D_m^{-1} \geq 0$. If this is the case, using Schür's complement, the entire matrix R_{mat} is positive definite when $R_m > 0$ and:

$$R_\sigma - \frac{1}{4}\beta - \frac{1}{4}\gamma R_m^{-1}\gamma > 0$$

Defining $\Omega := \left\{(q, p, x_m, x_l, \sigma) \in \mathbb{R}^{14} \;\middle|\; \dot{H}_\sigma = 0\right\}$ as the set all solutions converge to, the following is known inside that set:

$$\Omega \quad \Longrightarrow \quad \begin{cases} \frac{\partial \Phi_m}{\partial q_m} = -K_c x_m \quad \Longrightarrow \quad \dot{x}_m = 0 \\ \frac{\partial \Phi_\sigma}{\partial \sigma} = 0 \quad \Longrightarrow \quad \sigma = 0 \\ \dot{q}_l, \dot{q}_p = 0 \quad \Longrightarrow \quad p_l, p_m = 0 \quad \Longrightarrow \quad \dot{p}_l, \dot{p}_m = 0 \\ \frac{\partial \Phi_l}{\partial q_l} = 0 \quad \Longrightarrow \quad \tilde{q}_l = x_l \end{cases}$$

Then similarly to the previous section:

$$\dot{p}_l + \dot{p}_m = -\frac{\partial \Phi_m}{\partial q_m} = 0 \quad \Longrightarrow \quad x_m = 0 \quad \Longrightarrow \quad q_m = q_m^*$$

$$\dot{p}_l = \frac{\partial V}{\partial q_l} = 0 \quad \Longrightarrow \quad q_l = q_m = 0$$

showing that $(q, p, x_l, x_m, \sigma) = (\tilde{q}, 0, 0, 0, 0)$ is asymptotically stable. Similarly to the previous section, the PH-structure cannot be preserved. □

Results

The steady-state error is eliminated and convergence occurs in around 5 seconds. The control signals are still present but declining as the friction keeps the motors static. See figure 6.5. Although convergence takes longer than in the previous example, in this experiment the positions converge exactly to the set points. Oscillations smaller and damped quicker than the last example.

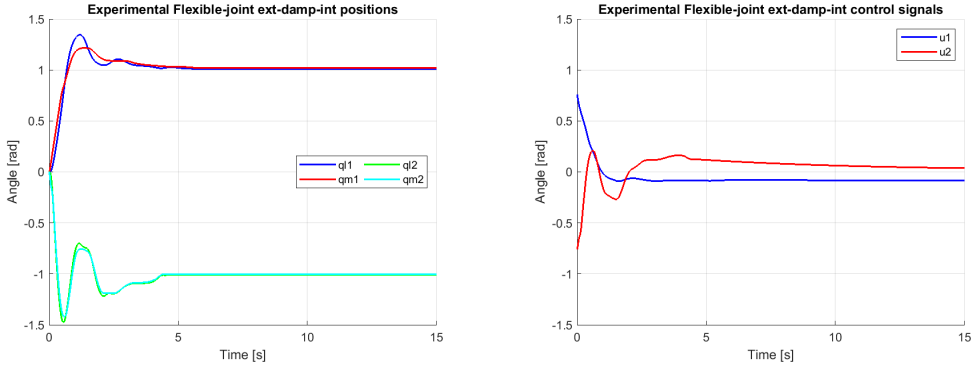

((a)) ((b))

Figure 6.5: Experimental positions and control signals for saturated control, with damping on the links and double integral action, on flexible-joint arm

The results of the control laws are interesting, but the only results that are shown are those of setpoint regulation from different initial conditions. To find out more about the robustness of the controller, the next chapter will see what happens when the arm is disturbed whilst at its set point.

Chapter 7

External disturbance rejection

In this chapter the flexible control laws will be tested to determine how fast they re-stabilize the arm after an external disturbance. The external disturbance will be a push against the end of the arm.

LQR

The LQR takes around 20 seconds to stabilize the arm after an initial deflection of 0.25 rad. A large number of oscillations are seen both in the positions and control signals. See figure 7.2.

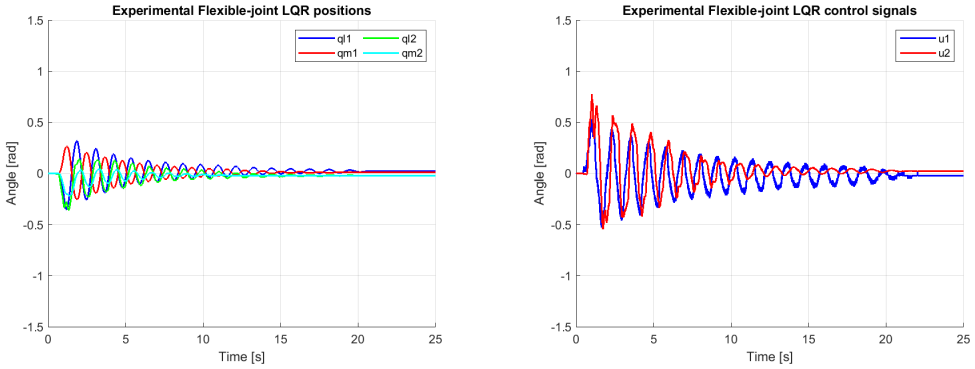

((a)) ((b))

Figure 7.1: Experimental positions and control signals for LQR, rejecting disturbance in flexible-joint arm

PI control

It can be seen that the PI control law stabilizes the arm at the same rate the LQR does. The control signals are however much smaller. The PI control law cuts the oscillation to a certain point after which the control signals are not large enough to overcome the sticking point of the motors, the links are then damped by the natural friction only.

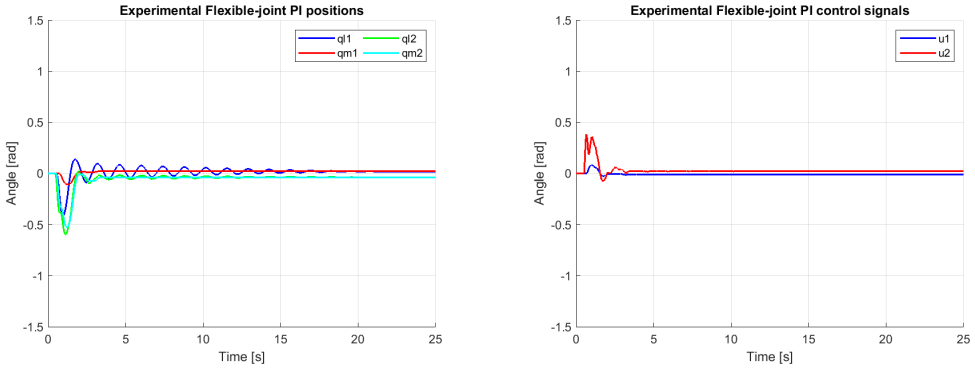

((a)) ((b))

Figure 7.2: Experimental positions and control signals for PI control, rejecting disturbance in flexible-joint arm

PI control with damping on the links

The PI control with damping on the links once again has excellent performance. The disturbance is rejected in under two seconds. The best results by a factor of 10. The control signal used is very large, exceeding the saturation limit. See figure 7.3.

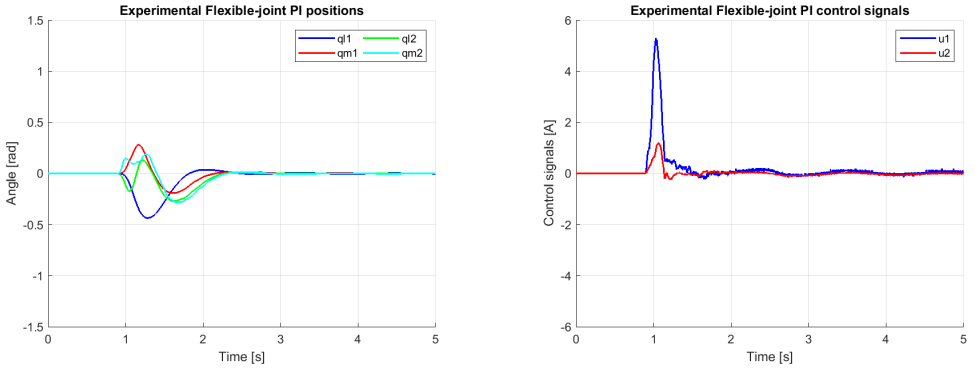

((a)) ((b))

Figure 7.3: Experimental positions and control signals for PI control with damping on the links, rejecting disturbance in flexible-joint arm

Saturated control without velocity measurements

The saturated control has very similar behavior to the normal PI control. It stops the large oscillations but the small oscillations are not affected. It leaves a relatively large steady state error. See figure 7.4.

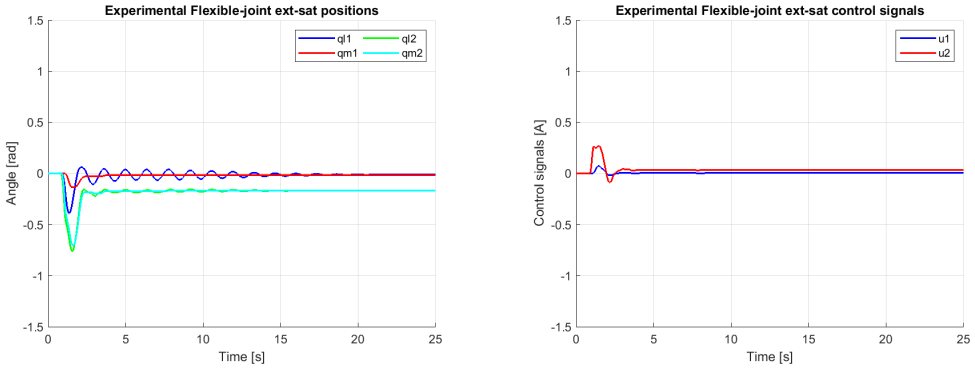

((a)) ((b))

Figure 7.4: Experimental positions and control signals for saturated PI control without position measurements, rejecting disturbance in flexible-joint arm

Saturated control with damping on the links without velocity measurements

The saturated control performs slightly better but the control signals show this is not because of its input. The controller only gives a signal for the first 7 seconds, after this the deflections become too small to register.

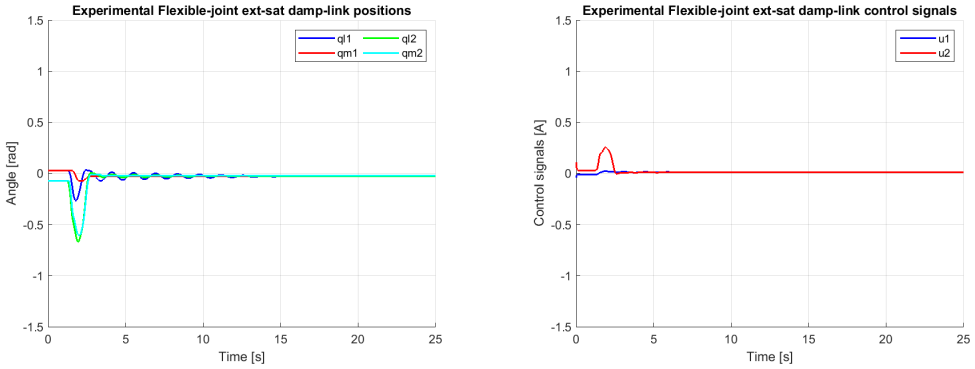

((a)) ((b))

Figure 7.5: Experimental positions and control signals for saturated PI with damping on the links, rejecting disturbance in flexible-joint arm

Chapter 8

Discussion and future research

This thesis provides the proof for asymptotic stability of different kinds of controllers for planar (flexible-joint) manipulators. It shows that considering linear damping might provide more adaptability when considering passivity-based methods in the port-Hamiltonian framework. Additionally, it introduces naturally saturated control for the specific system.

From the experimental results it becomes obvious that most control laws (barring the law with double integral action) tested on the experimental set-up leave relatively large steady-state error. It is likely that there is a sticking point in the engine which is hard to overcome at low speeds. This hints at the explanation that a non-linear friction model (such as coulomb friction) would explain the natural damping better than the current linear one. The experimental set-up could be researched further to determine a better model for the friction.

In the results it can be seen that in the rigid case, the non-linear control laws show little to no improvement over the linear quadratic regulator. However, the flexible-joint set-up is forced to its desired equilibrium faster than the LQR with all non-linear control laws. The non-linear PI controller with damping on the links yields the best results. When the velocity measurements are sacrificed, this negatively impacts the performance of the controller.

Several opportunities for research related to the work in this thesis remain:

- The effects of non-linear frictions on the preservation of mechanical structure under different control laws can be investigated. This research assumed linear friction although the experimental results show a non-linear model for the friction would be more accurate. The effectivity of controls based on the dynamics with linear friction suggest that similar techniques might work for non-linear models of friction.
- The technique of developing saturated control laws could be generalized to a class of systems. It is probable that saturated control will work on additional kinds of dynamical systems. However, the requirements on these systems need to be formalized.

Bibliography

[1] Pablo Borja, Rafael Cisneros, and Romeo Ortega. A constructive procedure for energy shaping of porthamiltonian systems. *Automatica*, 72:230–234, 2016.

[2] Stuart Bennett. A brief history of automatic control. *IEEE Control Systems*, 16 (3):17–25, 1996.

[3] Richard C Dorf and Robert H Bishop. *Modern control systems*. Pearson, 2011.

[4] James Clerk Maxwell et al. I. on governors. *Proceedings of the Royal Society of London*, 16:270–283, 1868.

[5] Nicolas Minorsky. Directional stability of automatically steered bodies. *Journal of the American Society for Naval Engineers*, 34(2):280–309, 1922.

[6] Daniel Alonzo Dirksz. *Robust energy- and power-based control design: Port-Hamiltonian and Brayton-Moser systems*. PhD thesis, 2011. Relation: https://www.rug.nl/ Rights: Dirksz, Daniel Alonzo.

[7] BM Maschke and AJ Van Der Schaft. Port-controlled hamiltonian systems: modelling origins and systemtheoretic properties. In *Nonlinear Control Systems Design 1992*, pages 359–365. Elsevier, 1993.

[8] AJ van der Schaft. *L2-gain and passivity techniques in nonlinear control*, volume 2. Springer, 2000.

[9] Hassan K Khalil. Nonlinear systems. *Prentice-Hall, New Jersey*, 2(5):5–1, 1996.

[10] Mathukumalli Vidyasagar. *Nonlinear systems analysis*, volume 42. Siam, 2002.

[11] Jean-Jacques E Slotine, Weiping Li, et al. *Applied nonlinear control*, volume 199. Prentice hall Englewood Cliffs, NJ, 1991.

[12] Jan C Willems. Dissipative dynamical systems part ii: Linear systems with quadratic supply rates. *Archive for rational mechanics and analysis*, 45(5):352–393, 1972.

[13] Romeo Ortega, Arjan J Van Der Schaft, Iven Mareels, and Bernhard Maschke. Putting energy back in control. *IEEE Control Systems*, 21(2):18–33, 2001.

[14] David Hill and Peter Moylan. The stability of nonlinear dissipative systems. *IEEE Transactions on Automatic Control*, 21(5):708–711, 1976.

[15] Romeo Ortega and Eloisa Garcia-Canseco. Interconnection and damping assignment passivity-based control: A survey. *European Journal of control*, 10(5):432–450, 2004.

[16] Huibert Kwakernaak and Raphael Sivan. *Linear optimal control systems*, volume 1. Wiley-Interscience New York, 1972.

[17] Mark W Spong. Modeling and control of elastic joint robots. *Journal of dynamic systems, measurement, and control*, 109(4):310–318, 1987.

[18] Alessandro De Luca. Flexible robots. *Encyclopedia of Systems and Control*, pages 451–458, 2015.

[19] H Jardón-Kojakhmetov, M Muñoz-Arias, and Jacquelien MA Scherpen. Model reduction of a flexible-joint robot: a port-hamiltonian approach. *IFAC-PapersOnLine*, 49(18):832–837, 2016.

[20] Brian Armstrong-Helouvry. Stick-slip arising from stribeck friction. In *Robotics and Automation, 1990. Proceedings., 1990 IEEE International Conference on*, pages 1377–1382. IEEE, 1990.